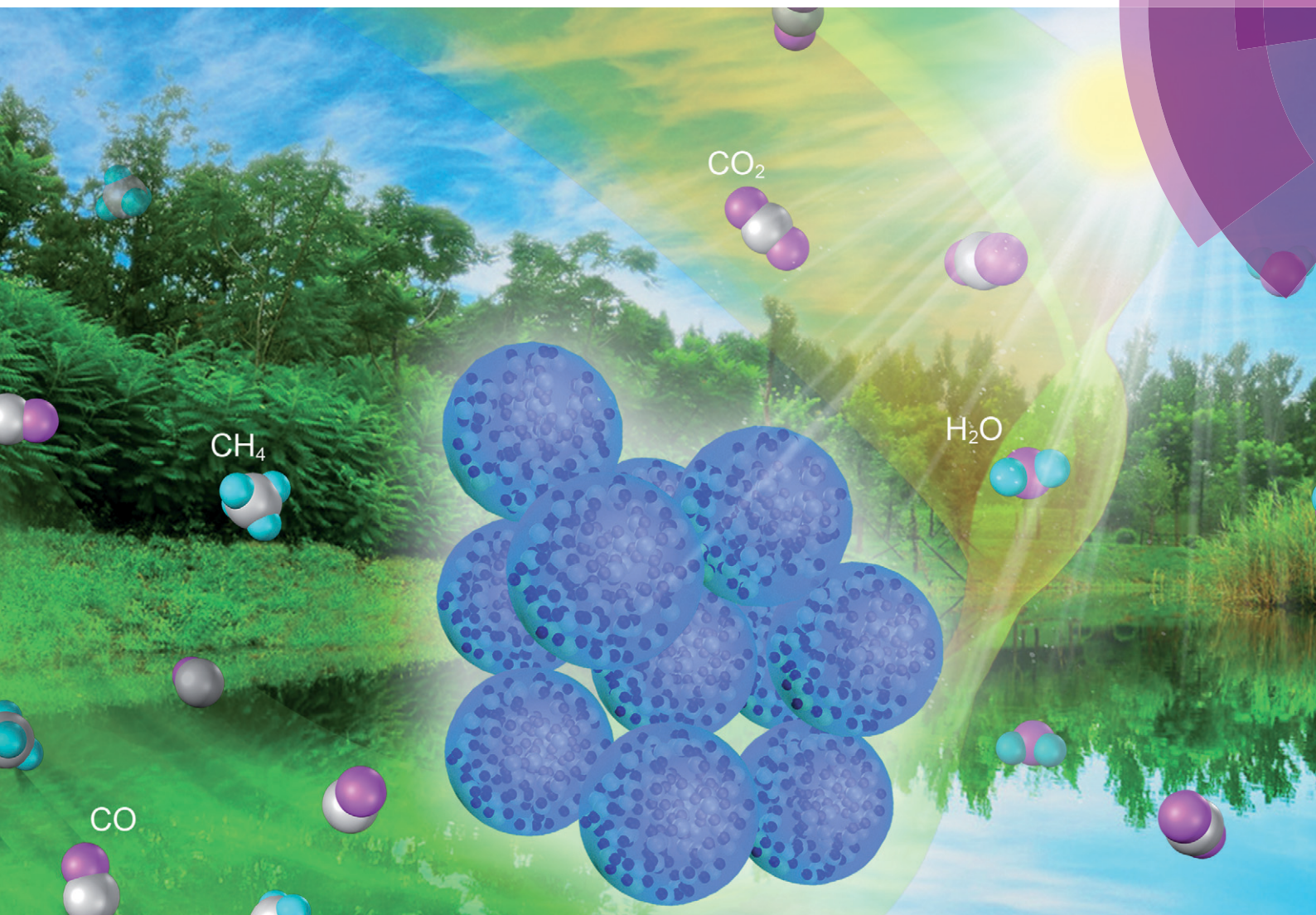


Catalysis Science & Technology

www.rsc.org/catalysis



Themed issue: Catalytic Conversion and Use of Carbon Dioxide for Value-Added Organics

ISSN 2044-4753



PAPER

Ying Li *et al.*

CO₂ photoreduction with H₂O vapor by porous MgO–TiO₂ microspheres: effects of surface MgO dispersion and CO₂ adsorption–desorption dynamics

Catalysis Science & Technology

www.rsc.org/catalysis



Chemical Fixation

Homogeneous
Hydrogenation

Methanol

ISSN 2044-4753



ROYAL SOCIETY
OF CHEMISTRY

MINIREVIEW

Liang-Nian He *et al.*

Homogeneous hydrogenation of carbon dioxide to methanol

Catalysis Science & Technology

A multidisciplinary journal focussing on all fundamental science and technological aspects of catalysis

www.rsc.org/catalysis

The Royal Society of Chemistry is the world's leading chemistry community. Through our high impact journals and publications we connect the world with the chemical sciences and invest the profits back into the chemistry community.

IN THIS ISSUE

ISSN 2044-4753 CODEN CSTAGD 4(6) 1467-1838 (2014)



Cover

See Ying Li *et al.*, pp. 1539–1546.
Image reproduced by permission of Ying Li from *Catal. Sci. Technol.*, 2014, 4, 1539.



Inside cover

See Liang-Nian He *et al.*, pp. 1498–1512.
Image reproduced by permission of Liang-Nian He from *Catal. Sci. Technol.*, 2014, 4, 1498.

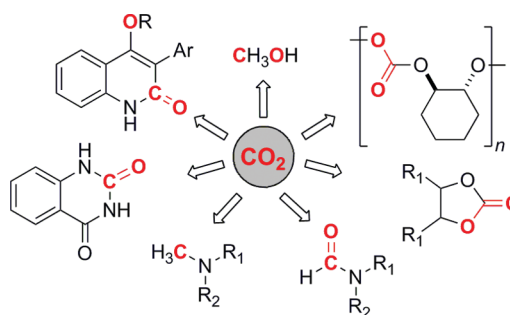
EDITORIAL

1481

Catalytic conversion and use of carbon dioxide

Arjan W. Kleij^{*}

Welcome to this themed issue describing the latest advances made in the area of CO₂ catalysis and conversion with a focus on its use in organic synthesis.



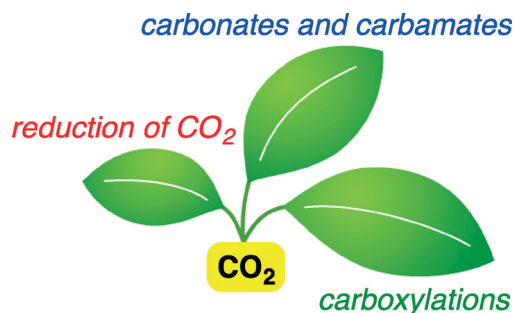
PERSPECTIVES

1482

Recent progress in catalytic conversions of carbon dioxide

Chihiro Maeda,^{*} Yuki Miyazaki and Tadashi Ema^{*}

The latest progress in chemical conversions of CO₂ into useful compounds is overviewed.



Editorial staff

Managing editor

Jamie Humphrey

Deputy editor

Fiona McKenzie

Senior publishing editor

Andrew Shore

Development editor

Guy Jones

Publishing editors

Emma Cooper, Rachel Cooper, Debora Giovanelli, Caroline Knapp, Helen Lunn, Amy Middleton-Gear, Kirsty Muirhead, Michael Parkin, Anisha Ratan, Elizabeth Woodhouse

Publishing assistants

Judy Allen, Ella Mitchell

For queries about submitted articles please contact Andrew Shore, Senior publishing editor, in the first instance. E-mail catalysis@rsc.org

For pre-submission queries please contact Jamie Humphrey, Managing editor.

E-mail catalysis-rsc@rsc.org

Catalysis Science & Technology (print: ISSN 2044-4753; electronic: ISSN 2044-4761) is published monthly by the Royal Society of Chemistry, Thomas Graham House, Science Park, Milton Road, Cambridge, UK CB4 0WF.

All orders, with cheques made payable to the Royal Society of Chemistry, should be sent to RSC, Order Department, Royal Society of Chemistry, Thomas Graham House, Science Park, Milton Road, Cambridge, CB4 0WF, UK
Tel +44 (0)1223 432398; E-mail orders@rsc.org

2014 Annual (print + electronic) subscription price: £1643; US\$2876. 2014 Annual (electronic) subscription price: £1561; US\$2732. Customers in Canada will be subject to a surcharge to cover GST. Customers in the EU subscribing to the electronic version only will be charged VAT.

If you take an institutional subscription to any RSC journal you are entitled to free, site-wide web access to that journal. You can arrange access via Internet Protocol (IP) address at www.rsc.org/ip. Customers should make payments by cheque in sterling payable on a UK clearing bank or in US dollars payable on a US clearing bank.

US Postmaster: send address changes to Catalysis Science & Technology, c/o Mercury Airfreight International Ltd., 365 Blair Road, Avenel, NJ 07001. All despatches outside the UK by Consolidated Airfreight.

Advertisement sales: Tel +44 (0) 1223 432246; Fax +44 (0) 1223 426017; E-mail advertising@rsc.org

For marketing opportunities relating to this journal, contact marketing@rsc.org

Catalysis Science & Technology

A multidisciplinary journal focussing on all fundamental science and technological aspects of catalysis

www.rsc.org/catalysis

Editorial board

Co-Editors-in-chief

Piet van Leeuwen,
Institute of Chemical Research of
Catalonia (ICIQ), Spain
Noritaka Mizuno,
University of Tokyo, Japan

Javier Pérez-Ramirez, ETH Zürich,
Switzerland
Tsunehiro Tanaka,
Kyoto University, Japan

David Jackson,
University of Glasgow, UK
Axel Knop-Gericke,
Fritz Haber Institute of the
Max Planck Society, Germany
Johannes de Vries,
DSM Research/University of
Groningen, The Netherlands

Associate Editors

Paul Chirik,
Princeton University, USA
Paul Kamer,
University of St Andrews, UK

Members

Xinhe Bao, State Key Laboratory of
Catalysis, China
Christian Bruneau, Institut des
Sciences Chimiques de Rennes,
France

Advisory board

Isabel Arends, Delft University of
Technology, The Netherlands
Alfons Baiker, ETH Zurich, Switzerland
Robin Bedford, University of Bristol,
UK
Bhalchandra Bhanage, Institute of
Chemical Technology, Mumbai,
India
George Britovsek, Imperial College
London, UK
Bruno Chaudret, National Centre of
Scientific Research (CNRS), France
Michel Che, Université Pierre et Marie
Curie, France
Chien-Tien Chen, National Tsing Hua
University, Chinese Taipei
Matt Clarke, University of St Andrews,
UK
Christophe Copereit, ETH Zurich,
Switzerland
Avelino Corma, Valencia University,
Spain
Richard Crooks, The University of
Texas at Austin, USA
Ian Fairlamb, University of York, UK

Ben Feringa, University of Groningen,
The Netherlands
John Fossey, University of
Birmingham, UK
Greg Fu, California Institute of
Technology, USA
Bruce Gates, University of California,
USA
Gideon Grogan, University of York,
UK
Chris Hardacre, Queen's University
Belfast, UK
John Hartwig, University of Illinois,
USA
Graham Hutchings, University of
Cardiff, UK
Can Li, Dalian Institute of Chemical
Physics, China
Antoni Llobet, ICIQ, Spain
Guido Mul, Twente University, The
Netherlands
Kyoko Nozaki, University of Tokyo,
Japan

Steven Nolan, University of St
Andrews, UK
Robert M. Rioux, The Pennsylvania
State University, USA
Tito Scaiano, University of Ottawa,
Canada
James J. Spivey, Louisiana State
University, USA
Mizuki Tada, Nagoya University, Japan
Franklin Tao, University of Notre
Dame, USA
Nick Turner, Manchester University,
UK
Andy York, Johnson Matthey, UK
Francisco Zaera, University of
California, USA

Information for authors

Full details on how to submit material for publication in Catalysis Science & Technology are given in the Instructions for Authors (available from <http://www.rsc.org/authors>). Submissions should be made via the journal's homepage: <http://www.rsc.org/catalysis>.

Authors may reproduce/republish portions of their published contribution without seeking permission from the RSC, provided that any such republication is accompanied by an acknowledgement in the form: (Original Citation)–Reproduced by permission of the Royal Society of Chemistry.

This journal is © The Royal Society of Chemistry 2014. Apart from fair dealing for the purposes of research or private study for non-commercial purposes, or criticism or review, as permitted under the Copyright, Designs and

Patents Act 1988 and the Copyright and Related Rights Regulation 2003, this publication may only be reproduced, stored or transmitted, in any form or by any means, with the prior permission in writing of the Publishers or in the case of reprographic reproduction in accordance with the terms of licences issued by the Copyright Licensing Agency in the UK. US copyright law is applicable to users in the USA.

The Royal Society of Chemistry takes reasonable care in the preparation of this publication but does not accept liability for the consequences of any errors or omissions.

© The paper used in this publication meets the requirements of ANSI/NISO Z39.48–1992 (Permanence of Paper).

Registered Charity No. 207890.



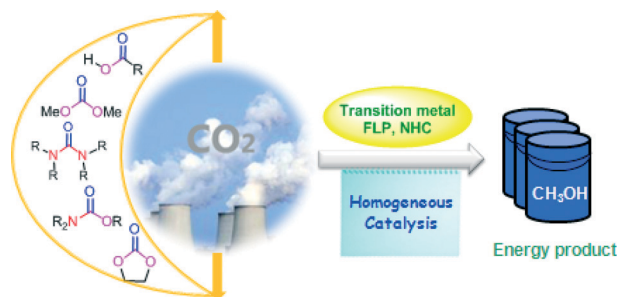
MINI REVIEWS

1498

Homogeneous hydrogenation of carbon dioxide to methanol

Yu-Nong Li, Ran Ma, Liang-Nian He* and Zhen-Feng Diao

Homogeneous catalytic hydrogenation of CO₂ into fuel-related products, e.g. methanol, is highlighted in combination with mechanistic understanding on a molecular level.

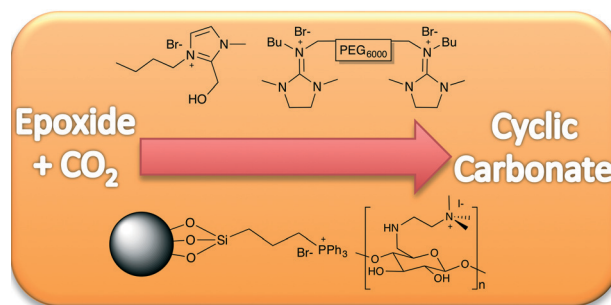


1513

Synthesis of cyclic carbonates from CO₂ and epoxides using ionic liquids and related catalysts including choline chloride–metal halide mixtures

Qing He, Jeremy W. O'Brien, Kayla A. Kitselman, Lindsay E. Tompkins, Gregory C. T. Curtis and Francesca M. Kerton*

In this mini-review, progress made in the use of ionic liquid catalysts and related systems for cycloaddition reactions of carbon dioxide with epoxides is described with the primary focus on results from the past eight years.



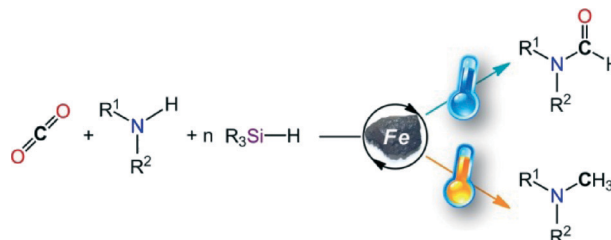
COMMUNICATIONS

1529

Iron-catalyzed hydrosilylation of CO₂: CO₂ conversion to formamides and methylamines

Xavier Frogneux, Olivier Jacquet and Thibault Cantat*

Catalytic hydrosilylation of CO₂ is an efficient and selective approach to form chemicals. Herein, we describe the first iron catalysts able to promote the reductive functionalization of CO₂ using hydrosilanes as reductants. Iron(II) salts supported by phosphine donors enable the conversion of CO₂ to formamide and methylamine derivatives under mild reaction conditions.

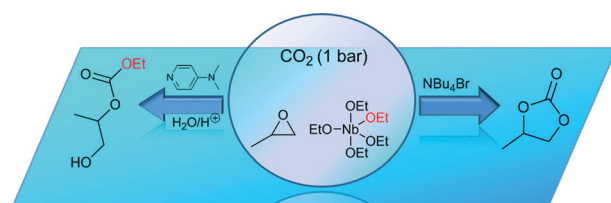


1534

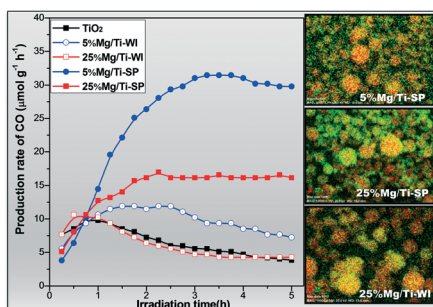
Nucleophile-directed selectivity towards linear carbonates in the niobium pentaethoxide-catalysed cycloaddition of CO₂ and propylene oxide

Barnali Dutta, Julien Sofack-Kreutzer, Amylia A. Ghani, Valerio D'Elia,* Jérémie D. A. Pelletier, Mirza Cokoja, Fritz E. Kühn* and Jean-Marie Basset

The reaction between CO₂ and propylene oxide in the presence of Nb(EtO)₅ and 4-dimethylaminopyridine leads to the formation of an acyclic carbonate through an unprecedented pathway.



1539

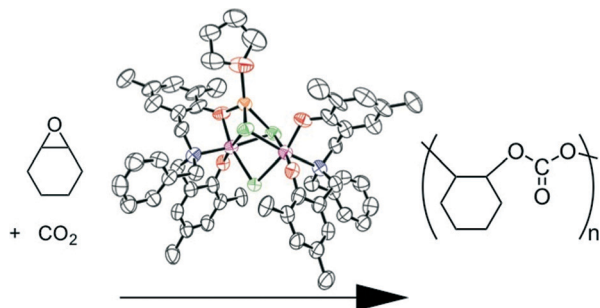


CO₂ photoreduction with H₂O vapor by porous MgO–TiO₂ microspheres: effects of surface MgO dispersion and CO₂ adsorption–desorption dynamics

Lianjun Liu, Cunyu Zhao, Daniel Pitts, Huilei Zhao and Ying Li*

Porous MgO–TiO₂ microspheres prepared by a one-pot spray pyrolysis method significantly enhance the activity and stability in CO₂ photoreduction with water vapor.

1547

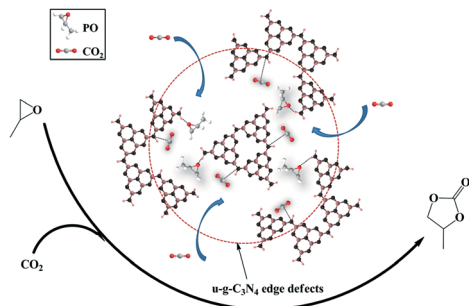


Chromium(III) amine-bis(phenolate) complexes as catalysts for copolymerization of cyclohexene oxide and CO₂

Hua Chen, Louise N. Dawe and Christopher M. Kozak*

Chromium complexes of tri- and tetradentate amine-bis(phenolate) ligands in combination with chloride, azide or DMAP nucleophiles are effective catalysts for the copolymerization of CO₂ with cyclohexene oxide to give polycarbonates.

1556

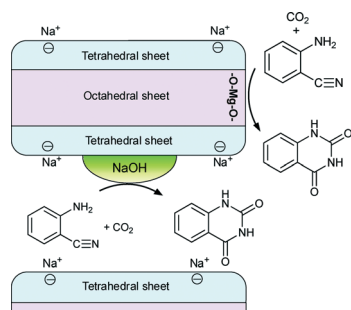


Urea-derived graphitic carbon nitride as an efficient heterogeneous catalyst for CO₂ conversion into cyclic carbonates

Qian Su, Jian Sun, Jinqun Wang, Zifeng Yang, Weiguo Cheng* and Suojiang Zhang*

Urea-derived graphitic carbon nitrides (u-g-C₃N₄) were prepared under different temperatures as catalysts for CO₂ conversion into cyclic carbonates.

1563



Synthesis of quinazoline-2,4(1*H*,3*H*)-dione from carbon dioxide and 2-aminobenzonitrile using mesoporous smectites incorporating alkali hydroxide

Shin-ichiro Fujita, Masahiro Tanaka and Masahiko Arai*

Incorporation of alkali hydroxide into smectite significantly enhances the catalytic activity for the synthesis of quinazoline-2,4(1*H*,3*H*)-dione from carbon dioxide and 2-aminobenzonitrile, which has been ascribed to the formation of NaOH particles on the surface of the smectite layer.

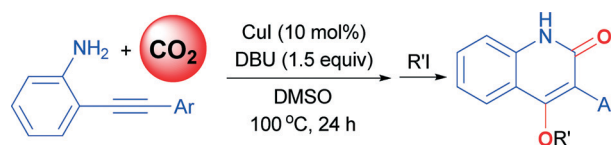
PAPERS

1570

Cu(I)-catalyzed chemical fixation of CO₂ with 2-alkynylaniline into 4-hydroxyquinolin-2(1H)-one

Chun-Xiao Guo, Wen-Zhen Zhang,* Si Liu and Xiao-Bing Lu

A copper(I)-catalyzed reaction of 2-alkynylaniline with CO₂ using DBU as base to produce 4-hydroxyquinolin-2(1H)-one derivatives in moderate to good yield is presented.

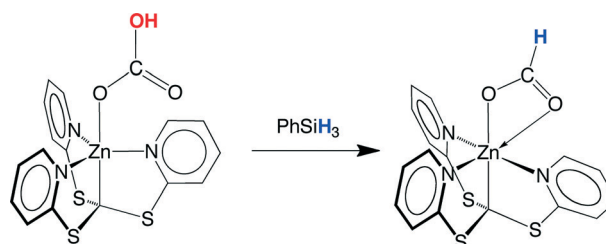


1578

Reduction of bicarbonate and carbonate to formate in molecular zinc complexes

Wesley Sattler and Gerard Parkin*

The zinc bicarbonate complex, [κ⁴-Tptm]ZnOCO₂H, is reduced by PhSiH₃ to give the formate derivative, [κ⁴-Tptm]ZnO₂CH, via a sequence that involves release of CO₂ followed by insertion into a zinc-hydride bond.

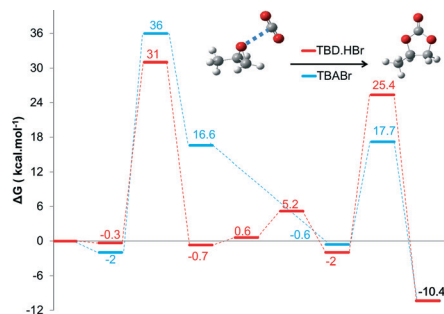


1585

Theoretical study on the chemical fixation of carbon dioxide with propylene oxide catalyzed by ammonium and guanidinium salts

Stéphanie Foltran, Raphaël Mereau and Thierry Tassaing*

A catalytic mechanism involved in the cycloaddition of propylene oxide onto CO₂ catalyzed by ammonium and guanidinium salts is proposed.

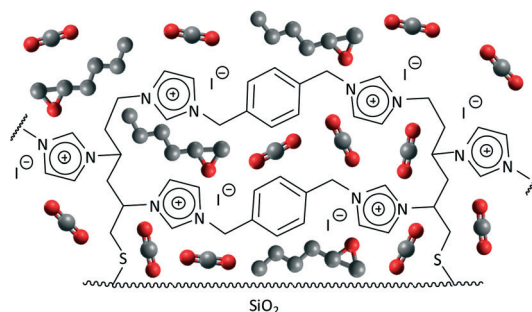


1598

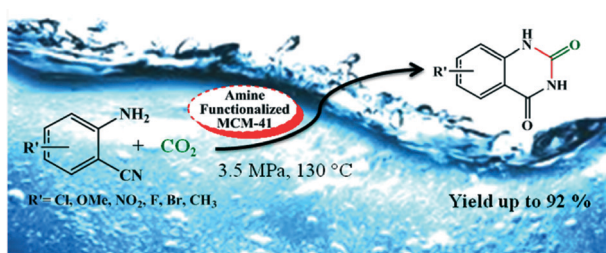
Synthesis and high-throughput testing of multilayered supported ionic liquid catalysts for the conversion of CO₂ and epoxides into cyclic carbonates

Paola Agrigento, Syed M. Al-Amsyar, Benjamin Sorée, Masoumeh Taherimehr, Michelangelo Gruttadauria,* Carmela Aprile* and Paolo P. Pescarmona*

Multilayered covalently supported ionic liquid catalysts achieve excellent TON and productivity in the reaction of CO₂ with various epoxides to produce cyclic carbonates.



1608

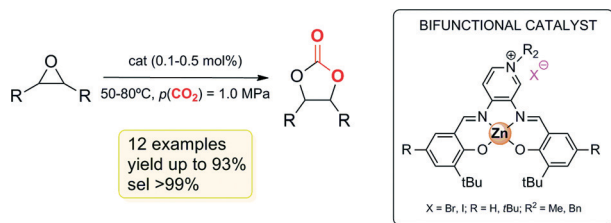


Amine functionalized MCM-41: an efficient heterogeneous recyclable catalyst for the synthesis of quinazoline-2,4(1*H*,3*H*)-diones from carbon dioxide and 2-aminobenzonitriles in water

Deepak B. Nale, Surjyakanta Rana, Kulamani Parida* and Bhalchandra M. Bhanage*

Covalently linked amine functionalized MCM-41 was investigated as an efficient catalyst for the synthesis of various quinazoline-2,4(1*H*,3*H*)-dione derivatives from 2-aminobenzonitriles and carbon dioxide in water.

1615

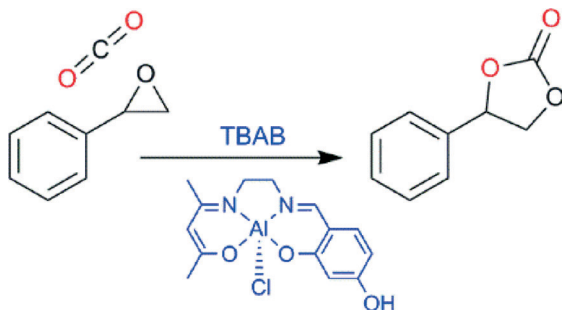


Easily accessible bifunctional Zn(salpyr) catalysts for the formation of organic carbonates

C. Martin, C. J. Whiteoak, E. Martin, M. Martínez Belmonte, E. C. Escudero-Adán and A. W. Kleij*

Alkylated Zn(salpyr) complexes (salpyr = *N,N'*-bis[salicylidene]-3,4-pyridinediamine) were prepared and used as catalyst precursors for the formation of cyclic carbonates from a range of (functional) epoxides and CO_2 .

1622

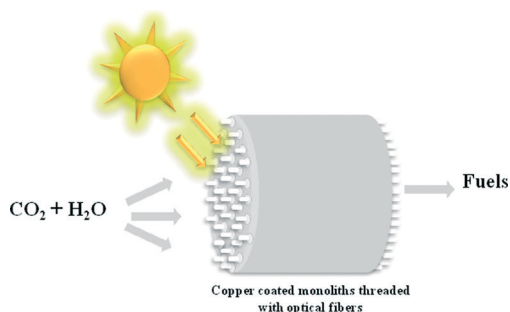


A single centre aluminium(III) catalyst and TBAB as an ionic organo-catalyst for the homogeneous catalytic synthesis of styrene carbonate

Somsak Supasitmongkol and Peter Styring*

Cyclic carbonate synthesis from an epoxide is achieved by sparging CO_2 at 1 bar into the solution using an aluminium/TBAB catalyst.

1631



Copper based TiO_2 honeycomb monoliths for CO_2 photoreduction

Oluwafunmilola Ola* and M. Mercedes Maroto-Valer

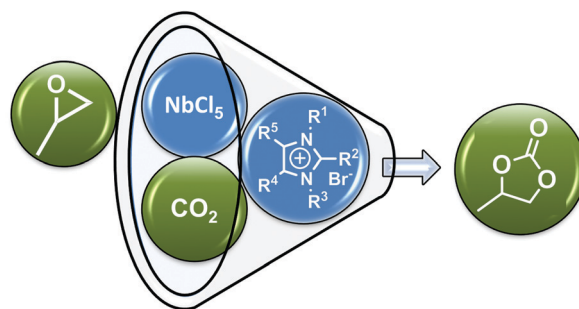
Copper based TiO_2 monolithic structures threaded with optical fibers exhibit better activity than pure TiO_2 for CO_2 reduction under visible or UV light irradiation.

1638

Niobium(v) chloride and imidazolium bromides as efficient dual catalyst systems for the cycloaddition of carbon dioxide and propylene oxide

M. E. Wilhelm, M. H. Anthofer, R. M. Reich, V. D'Elia, J.-M. Basset, W. A. Herrmann, M. Cokoja* and F. E. Kühn*

Imidazolium bromides combined with niobium(v) chloride were used as catalyst system for the reaction of CO₂ with epoxides to cyclic carbonates. The variation of the cation structure strongly affects the properties of the imidazolium salt and therefore the catalytic activity.

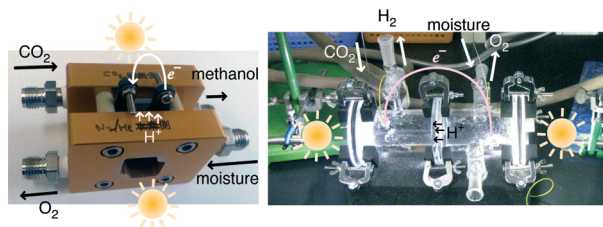


1644

Photocatalytic conversion of carbon dioxide into methanol in reverse fuel cells with tungsten oxide and layered double hydroxide photocatalysts for solar fuel generation

Motoharu Morikawa, Yuta Ogura, Naveed Ahmed, Shogo Kawamura, Gaku Mikami, Seiji Okamoto and Yasuo Izumi*

Photofuel cells comprising WO₃ and layered double hydroxide converted gaseous CO₂ into methanol whereas hydrogen was formed in the aqueous phase.

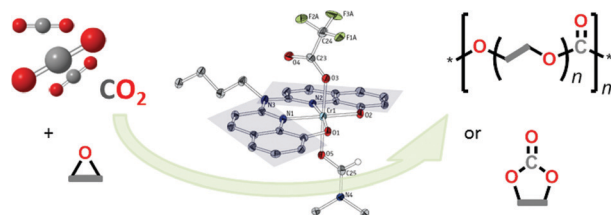


1652

Highly active Cr(III) catalysts for the reaction of CO₂ with epoxides

Sait Elmas, Muhammad A. Subhani, Marcus Harrer, Walter Leitner, Jörg Sundermeyer* and Thomas E. Müller*

This paper describes the synthesis and characterization of [Cr(babhq)OAc^F(EtOH)] (OAc^F = CF₃CO₂⁻) as well as the application of the complex as the catalyst in the reaction of CO₂ with epoxides.

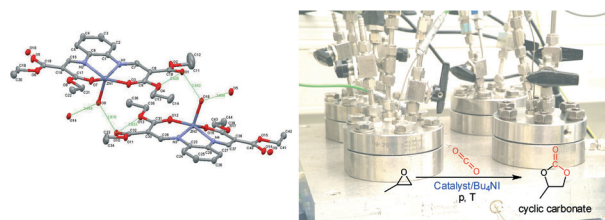


1658

New air-stable zinc complexes formed from cyanoacrylate- and methylenemalonate-based [N₂O₂]-ligands and their role as catalysts in epoxide-CO₂ coupling

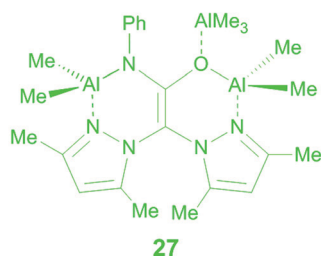
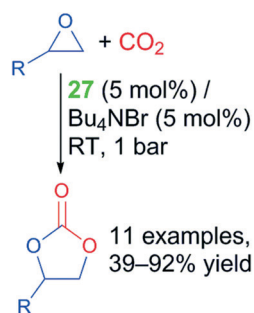
M. A. Fuchs, C. Altesleben, S. C. Staudt, O. Walter, T. A. Zevaco* and E. Dinjus

The synthesis of a range of zinc complexes based on ligands displaying an N₂O₂-framework with cyanoacrylate and/or malonate functionality is presented.



PAPERS

1674



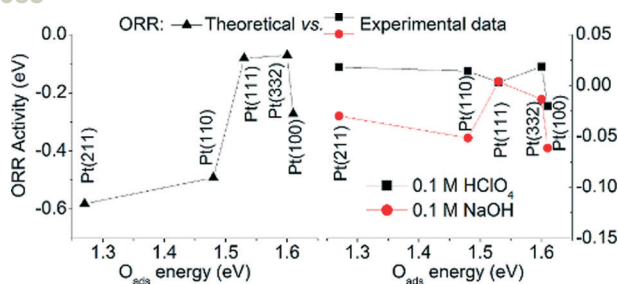
Synthesis of cyclic carbonates catalysed by aluminium heteroscorpionate complexes

José A. Castro-Osma, Carlos Alonso-Moreno, Agustín Lara-Sánchez, Javier Martínez, Michael North* and Antonio Otero*

A trimetallic aluminium complex catalyses the synthesis of cyclic carbonates from epoxides and CO_2 at room temperature and pressure.

PERSPECTIVES

1685

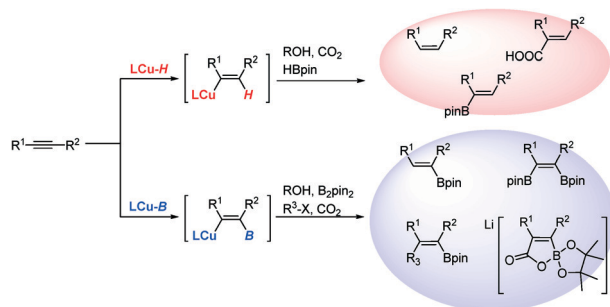


Oxygen reduction reaction at Pt single crystals: a critical overview

Ana M^a. Gómez-Marín, Rubén Rizo and Juan M. Feliu*

Oxygen reduction reaction: where do experimental and theoretical data coincide?

1699



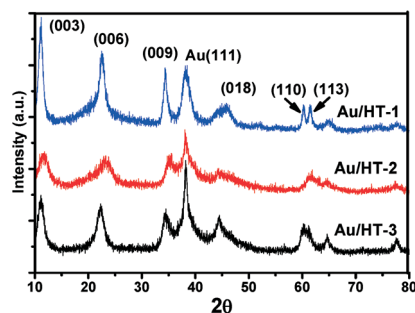
Regioselective transformation of alkynes catalyzed by a copper hydride or boryl copper species

Tetsuaki Fujihara, Kazuhiko Semba, Jun Terao and Yasushi Tsuji*

This review summarizes the transformation of alkynes using a copper hydride (Cu-H) or boryl copper (Cu-B) species as the active species, to afford multi-substituted alkenes that are potentially good intermediates in organic synthesis.

COMMUNICATIONS

1710



NaF regulated aqueous phase synthesis of aromatic amides and imines catalyzed by Au/HT

Qianqian Wang, Youquan Deng and Feng Shi*

An Au/HT catalyst was found to be an efficient heterogeneous catalyst for the coupling reaction of aromatic alcohols and amines.

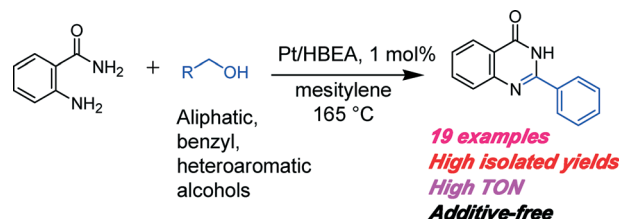
COMMUNICATIONS

1716

Direct synthesis of quinazolinones by acceptorless dehydrogenative coupling of *o*-aminobenzamide and alcohols by heterogeneous Pt catalysts

S. M. A. Hakim Siddiki,* Kenichi Kon, Abeda Sultana Touchy and Ken-ichi Shimizu

HBEA supported Pt metal nanoclusters effectively catalyze direct dehydrogenative synthesis of quinazolinones from *o*-aminobenzamide and alcohols under promoter-free conditions.

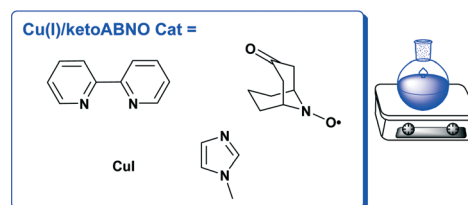


1720

Copper(I)/ketoABNO catalysed aerobic alcohol oxidation

Luke Rogan, N. Louise Hughes, Qun Cao, Laura M. Dornan and Mark J. Muldoon*

A copper(I)/ketoABNO aerobic catalyst system is highly effective for the oxidation of secondary alcohols, including unactivated aliphatic substrates. The effects of pressure and gas composition on catalyst performance are examined. The radical can be employed at low loadings and it is also amenable to immobilisation on to solid supports.

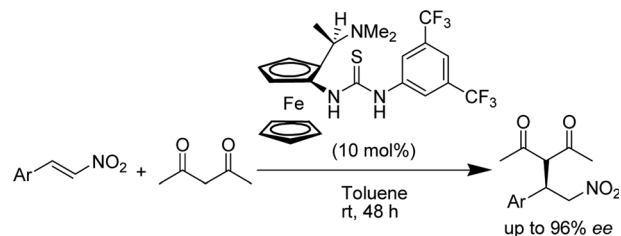


1726

Ferrocene as a scaffold for effective bifunctional amine–thiourea organocatalysts

Wei Yao, Ming Chen, Xueying Liu, Ru Jiang, Shengyong Zhang* and Weiping Chen*

This work demonstrates that ferrocene could be an excellent scaffold for chiral organocatalysts.

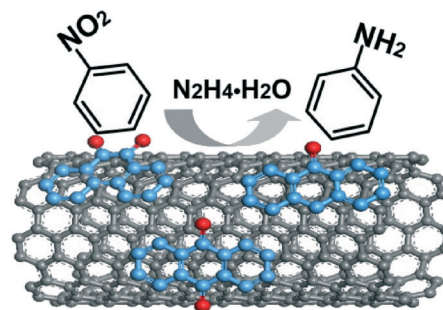


1730

Noncovalent functionalization of multi-walled carbon nanotubes as metal-free catalysts for the reduction of nitrobenzene

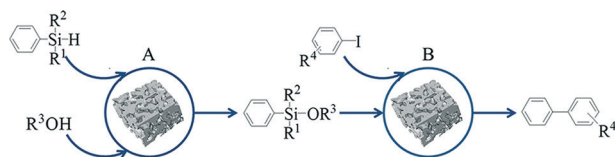
Xianmo Gu, Wei Qi, Shuchang Wu, Zhenhua Sun, Xianzhu Xu* and Dangsheng Su*

Multi-walled carbon nanotubes were functionalized noncovalently with small organic molecules containing specific ketonic carbonyl groups. The comparison of intrinsic activities for a series of catalysts indicates that carbonyl groups are active sites in the reduction of nitrobenzene.



COMMUNICATIONS

1734

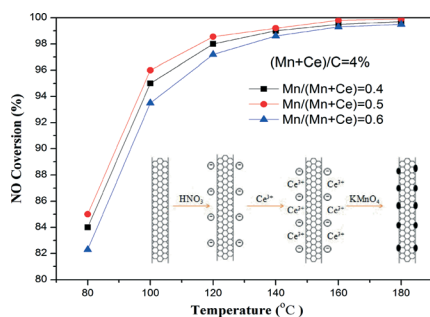


Nanoporous palladium catalyzed silicon-based one-pot cross-coupling reaction of aryl iodides with organosilanes

Zhiwen Li, Sha Lin, Lisha Ji, Zhonghua Zhang, Xiaomei Zhang* and Yi Ding*

One-pot cross-coupling of aryl iodides with organosilanes is realized using dealloyed nanoporous palladium as a sustainable and heterogeneous catalyst.

1738



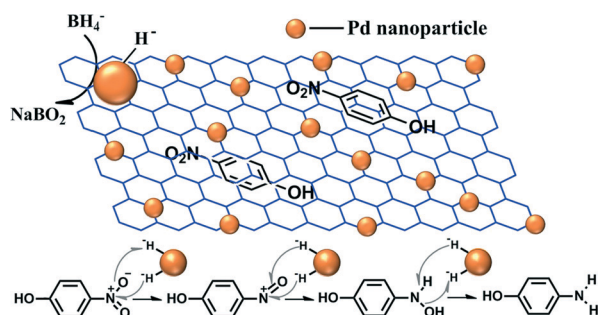
Low-temperature NO reduction with NH₃ over Mn-CeO_x/CNT catalysts prepared by a liquid-phase method

Xie Wang, Yuying Zheng,* Zhe Xu, Yi Liu and Xiaoli Wang

Mn-CeO_x/CNTs prepared by a liquid-phase method showed excellent low-temperature activity for NO reduction with NH₃.

PAPERS

1742

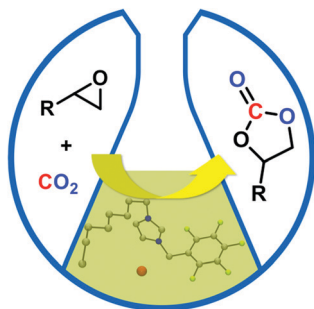


Catalytic hydrogenation of nitrophenols and nitrotoluenes over a palladium/graphene nanocomposite

Jingwen Sun, Yongsheng Fu,* Guangyu He, Xiaoqiang Sun* and Xin Wang*

A plausible mechanism for the reduction of *p*-nitrophenol catalyzed by a Pd/G catalyst in the presence of sodium borohydride.

1749



Cycloaddition of CO₂ and epoxides catalyzed by imidazolium bromides under mild conditions: influence of the cation on catalytic activity

Michael H. Anthofer, Michael E. Wilhelm, Mirza Cokoja,* Iulius I. E. Markovits, Alexander Pöthig, János Mink, Wolfgang A. Herrmann and Fritz E. Kühn

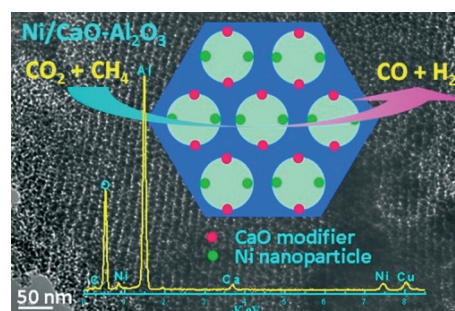
New imidazolium halide-based ionic liquids were employed as organocatalysts for the reaction of CO₂ and epoxides to cyclic carbonates at very mild reaction conditions. The substitution pattern influences the catalytic activity.

1759

Significant roles of mesostructure and basic modifier for ordered mesoporous Ni/CaO–Al₂O₃ catalyst towards CO₂ reforming of CH₄

Leilei Xu,* Zhichao Miao, Huanling Song, Wei Chen* and Lingjun Chou*

The significant roles of mesostructure and basic modifier in improving the catalytic performance of dry reforming were investigated.

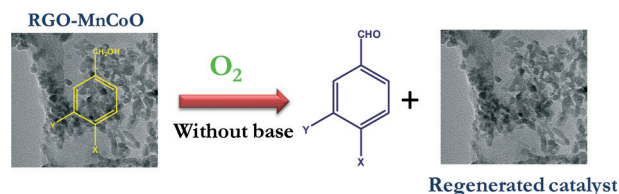


1771

Triple nanocomposites of CoMn₂O₄, Co₃O₄ and reduced graphene oxide for oxidation of aromatic alcohols

Ajay Jha, Dattakumar Mhamane, Anil Suryawanshi, Sameer M. Joshi, Parvez Shaikh, Narayan Biradar, Satishchandra Ogale* and Chandrashekhar V. Rode*

A triple nanocomposite of RGO with MnCoO provided anchoring sites for aromatic alcohols through π - π stacking near the metal redox center.

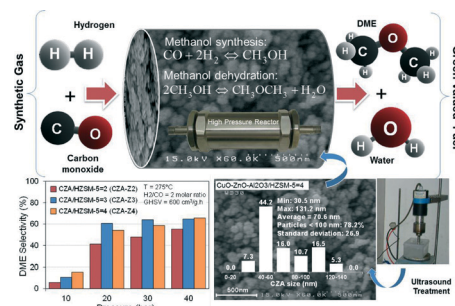


1779

Direct conversion of syngas to dimethyl ether as a green fuel over ultrasound-assisted synthesized CuO–ZnO–Al₂O₃/HZSM-5 nanocatalyst: effect of active phase ratio on physicochemical and catalytic properties at different process conditions

Reza Khoshbin and Mohammad Haghighi*

Hybrid co-precipitation–ultrasound synthesis of CuO–ZnO–Al₂O₃/HZSM-5 used in direct conversion of syngas to dimethyl ether as a green fuel.

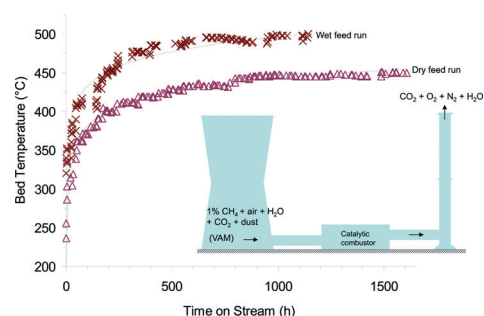


1793

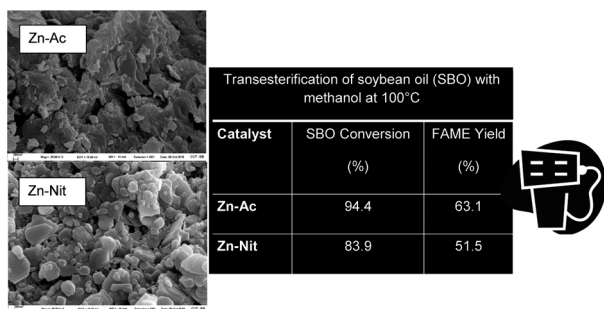
Catalytic combustion of ventilation air methane (VAM) – long term catalyst stability in the presence of water vapour and mine dust

Adi Setiawan, Jarrod Friggieri, Eric M. Kennedy, Bogdan Z. Dlugogorski and Michael Stockenhuber*

This paper presents long-term evaluation of catalyst stability and durability in the presence of water and coal mine dust.



1803

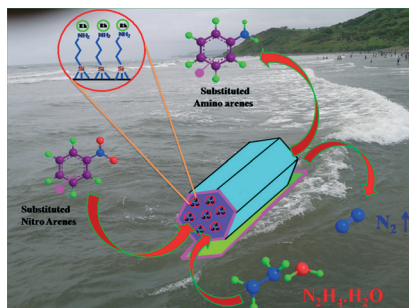


Synthesis of biodiesel from soybean oil using zinc layered hydroxide salts as heterogeneous catalysts

D. M. Reinoso, D. E. Damiani and G. M. Tonetto*

In this work, the transesterification of soybean oil with methanol using layered heterogeneous catalysts to produce biodiesel was studied.

1813

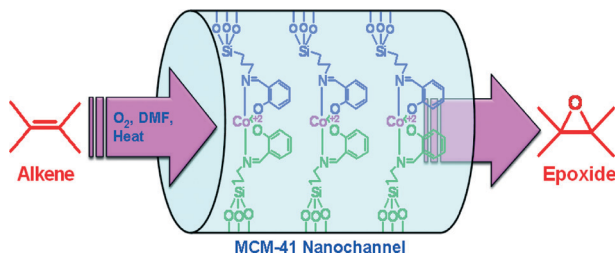


RhNPs/SBA-NH₂: a high-performance catalyst for aqueous phase reduction of nitroarenes to aminoarenes at room temperature

Saidulu Ganji, Siva Sankar Enumula, Ravi Kumar Marella, Kamaraju Seetha Rama Rao and David Raju Burri*

A RhNPs/SBA-NH₂ catalyst with <3 nm sized nanoparticles has been synthesized and used in the chemoselective hydrogenation of nitroarenes at room temperature in aqueous medium with N₂H₄·H₂O with high TOF.

1820

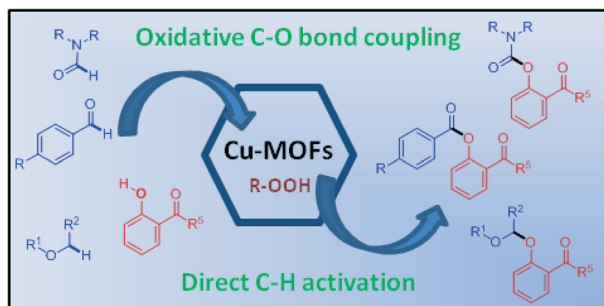


Catalytic olefin epoxidation over cobalt(II)-containing mesoporous silica by molecular oxygen in dimethylformamide medium

Susmita Bhunia, Sreyashi Jana, Debraj Saha, Buddhadeb Dutta and Subratanath Koner*

A cobalt(II) Schiff base complex has been anchored onto the surface of Si-MCM-41 to prepare a new catalyst. The catalyst is capable of catalyzing epoxidation reactions of olefinic compounds, including styrene and allyl alcohol, with molecular oxygen at atmospheric pressure in DMF medium.

1829



Cu-MOFs as active, selective and reusable catalysts for oxidative C-O bond coupling reactions by direct C-H activation of formamides, aldehydes and ethers

I. Luz, A. Corma* and F. X. Llabrés i Xamena*

Cu-MOFs are highly active, stable and recyclable catalysts for oxidative C-O coupling reactions involving direct activation of C-H bonds.

Catalytic combustion of ventilation air methane (VAM) – long term catalyst stability in the presence of water vapour and mine dust†

Cite this: *Catal. Sci. Technol.*, 2014, 4, 1793

Adi Setiawan,^{ab} Jarrod Friggieri,^a Eric M. Kennedy,^a Bogdan Z. Dlugogorski^{ac} and Michael Stockenhuber^{*a}

In this paper, we report new insights into the deactivation phenomenon of palladium based catalysts for catalytic combustion of ventilation air methane (VAM). It was found that the primary factor responsible for low temperature catalyst deactivation is the water vapour present in the feed stream. The influence of water vapour on VAM was examined by comparing the properties of fresh catalysts with catalysts following over 1000 h reaction time-on-stream. The techniques applied to characterize the catalysts included TPD, XRD, N₂-isotherm adsorption, H₂-chemisorption and XPS analyses. Alternating between dry and water vapour-saturated VAM feed disclosed ca. 50% reversible drop in activity. XPS analysis suggests an absence of a palladium hydroxide phase during the initial 2 h on stream, although prolonged exposure to the reactant leads to the formation of palladium hydroxide, which appears to match the progressive deactivation of the Pd/Al₂O₃ catalyst. Introduction of VAM dust (a mixture of fine coal, CaCO₃ and aluminosilicate particles) causes a variation in catalytic activity originating from coal-dust ignition and the effect of chloride on the surface of the catalyst. In the presence of these inhibiting agents, an average methane conversion of higher than 75% over 1100 h was achieved at reaction temperatures below 600 °C.

Received 28th January 2014,
Accepted 27th February 2014

DOI: 10.1039/c4cy00120f

www.rsc.org/catalysis

Introduction

Concerns over the rising concentration of greenhouse gases in the atmosphere have generally focused on carbon dioxide, although there is a growing emphasis on lowering methane emissions. Methane has been assigned a CO₂ greenhouse gas warming potential (GWP) of 25 over a 100 year time horizon,¹ and the conversion of CH₄ to CO₂ is considered as a potentially viable approach to reduce net emissions of greenhouse gases. Underground ventilation air systems in “gassy” coal mines contribute significantly to net methane emissions, although the concentration of methane in the ventilation air stream is typically below 1%. The high volumetric flow rates (typically 300 m³ s⁻¹) and the subsequent net discharge of significant quantities of methane have generated interest in developing technologies to reduce VAM emissions.² As reported in the

literature,^{3,4} besides air and methane, the VAM stream usually contains water (relative humidity = 70–100%), CO₂ (<2.5%), coal dust and others particles (such as calcium oxides, iron oxides, clay and quartz in a dust loading range of 0.1–4.5 mg m⁻³). It may also contain traces of CO, C₂H₆ (higher hydrocarbons), He, H₂, HCN, NH₃, NO_x, H₂S, and SO₂ (organic sulphur compounds).

Basically, VAM mitigation and utilization technologies are classified into two categories, ancillary uses and principal uses.^{5,6} For the ancillary uses, the VAM gas is used as combustion air for boilers, turbines and internal combustion engines while for principal uses the VAM is oxidized in a reactor to burn methane emission as well as produce energy. One potential technological solution for treatment of ventilation air methane (VAM) is catalytic combustion, where methane is oxidized to carbon dioxide on a catalytically active solid surface. This flameless combustion is ideal for highly diluted air-methane streams, such as VAM, as the concentration of methane is outside the typical flammability range of methane in air. Production of NO_x is essentially absent and the reaction temperature is relatively low (generally below 500 °C).

The catalytic oxidation of methane at low temperatures has been extensively investigated, especially over Pd and Pt based catalysts. A comprehensive review of methane oxidation over noble metal based catalysts agrees that the supported Pd

^a Priority Research Centre for Energy (PRCfE), Discipline of Chemical Engineering, School of Engineering, the University of Newcastle, Callaghan, NSW, 2308, Australia. E-mail: Michael.Stockenhuber@newcastle.edu.au

^b Jurusan Teknik Mesin, Fakultas Teknik, Universitas Malikussaleh, Reuleut, Aceh Utara, 24355, Indonesia

^c School of Engineering and Information Technology, Murdoch University, Murdoch, WA 6150, Australia

† Electronic supplementary information (ESI) available. See DOI: 10.1039/c4cy00120f

catalysts are the most active materials.⁷ However, palladium catalysts can be susceptible to poisoning by water vapour and other contaminants, which may result in severe deactivation when used in the catalytic combustion of VAM. Many recent investigations are focused on catalyst modifications which aim to enhance the durability of catalysts, especially developing resistance against water, sulfur compounds and particulates, as well as enhancing the absolute activity of the catalyst.⁷

Although it is well recognised that water vapour strongly inhibits the activity of catalysts, the mechanism of catalyst deactivation is uncertain.⁸ Some earlier studies reported that the water produced by the reaction significantly inhibits the activity of Pd/Al₂O₃ at lower temperatures due to competition with methane for active sites.^{9–11} Furthermore, irreversible deactivation can be induced by the presence of water vapour where the active site (PdO) transforms into a less active site (palladium hydroxide).^{9–12} The rate of Pd/Al₂O₃ catalyst deactivation in the presence of water, either present in the feed (such as the case in VAM) or produced in the catalytic combustion reaction, is heavily dependent on the reaction temperature.^{10,12} The inhibiting effect of water is more significant at lower temperatures, becoming less apparent at temperatures higher than 450 °C.¹⁰ Ciuparu *et al.* suggested that the hydroxyl groups produced by the reaction are bound strongly on the surface and when additional external water is introduced, the surface becomes saturated and the rate of desorption of water from the surface of the catalyst is slowed due to the high concentration of water vapour in the feed and product streams.¹³ Recent work by Schwartz *et al.* proposed an alternative explanation regarding deactivation of palladium supported on various metal oxides.^{8,14} They suggested that hydroxyl groups formed during the reaction accumulate on the catalyst support and inhibit the rate of exchange of oxygen between the support and PdO,¹⁴ a process which is necessary for surface reaction. This accumulation of hydroxyl groups prevents the migration of oxygen from the support to the Pd active site, as well as reducing the availability of oxygen involved in the oxidation of methane.⁸ Clearly, the primary mechanisms leading to deactivation are contentious, as it is possible that hydroxyls form on both the Pd site and the support in a high concentration⁸ and deactivation can potentially originate from the surface on either the support or palladium. Recently, Di Carlo and co-workers reported improved tolerance against water poisoning in catalytic combustion of methane over palladium catalysts by using a support which inhibited or delayed the reaction between Pd and H₂O,¹⁵ however no long time stability test results were reported.

The application of a catalytic process for VAM abatement requires long-term evaluation of the catalyst stability and durability under humid feed conditions. There are a limited number of reports on the hydrothermal stability tests of supported palladium catalysts. Yamamoto and Uchida reported longer-lasting hydrocarbon oxidation activity over Pt and Pd supported on alumina for lean-burn natural gas engine exhausts¹⁶ where the total hydrocarbon conversion dropped from 80% to 50% within 2500 h at 385 °C. Enhanced hydrothermal stability data during 3200 h methane oxidation at 600 °C were published recently by

Liu and co-workers.¹⁷ Hydrothermal stability of the catalyst was improved by optimizing the Ni/Al ratio for Ni supported alumina catalysts. Notwithstanding, stability data were not reported at reaction temperatures less than 600 °C nor the effect of CO₂ on the feed for long term catalyst stability tests. In addition, to our knowledge, there is no literature reporting on the effect of coal mine dust on the catalytic combustion of ventilation air methane.

In this paper, we report the effect of water and coal mine dust present on supported palladium catalysts during the catalytic combustion of a surrogate VAM gas. Attempts to improve the resistance of catalysts are explored by determining the differences in the physical and chemical characteristics of this catalyst (fresh and following long term activity testing). The stability of the Pd catalysts is evaluated for a long term activity under simulated ventilation air methane (where the feed contains components such as CH₄, CO₂, H₂O and air) in order to understand the deactivation phenomenon of the Pd/Al₂O₃ catalyst over a long period of time. The effect of coal mine dust is assessed by adding it to the catalyst and noting any effect it has on catalyst activity and stability. The combustion tests are operated under conditions where the level of methane conversion is maintained at or above 90% by increasing the catalyst bed temperature.

Experimental

Catalyst preparation

A catalyst containing 1.2 wt% Pd/Al₂O₃ was prepared by wet impregnation of an alumina (γ and δ Al₂O₃, Chem-Supply) support with an aliquot of Pd(II) nitrate solution (10 wt% in 10 wt% nitric acid, Sigma-Aldrich) mixed using a mortar and pestle. Water was added drop-wise while mixing, until a paste was formed. The resulting paste was dried in an oven at 110 °C for approximately 20 h. The dried catalyst was then ground, pressed and sieved to 250–400 μ m. A tubular fixed-bed reactor was used for calcination of a dried solid catalyst in air at 500 °C for 1 h followed by purging in helium for 30 min. For activation, the sample was reduced in H₂ at 300 °C for approximately 2 h and subsequently purged with helium while slowly heating the catalyst to the desired reaction temperature. For long-term stability experiments, we used a commercially available 1.0 wt% Pd/Al₂O₃ (Sigma-Aldrich) and activated it in air at 500 °C for 4 h followed by purging in H₂ for 2 h.

Catalyst characterization

The surface area of the catalysts was measured by nitrogen adsorption at 77 K using a Gemini 11 2370 surface area analyzer. A Micromeritics 2910 AutoChem (Micromeritics Instruments Corp., USA) was used to assess the active particle size and metal dispersion by performing a number of H₂ pulse-chemisorptions. Temperature-programmed desorption (TPD) analysis was carried out using a purpose built TPD apparatus with a Pfeiffer Prisma quadrupole mass analyser for detection. Transmission electronic microscopy (TEM) images of the sample were captured using a JEOL 2100. The palladium

loading was quantified using a Varian 715-ES inductively coupled plasma optical emission spectrometer (ICP-OES). Powder X-Ray diffraction patterns of the catalysts and ventilation air dust were obtained using Cu K α radiation using a Philips X'Pert diffractometer. Diffractograms were collected in the 2θ angle range from 2° to 90° with the 0.008° 2θ step resolution.

For surface analysis, *ex situ* X-ray photoelectron spectroscopy (XPS) was carried out using monochromated Al K α (energy 1486.68 eV) radiation and the emitted photoelectrons were analyzed using an ESCALAB250Xi manufactured by Thermo Scientific, UK. To minimize the possibility of sample contamination, spent samples were immediately transferred into sealed containers after stopping the reaction by cooling in helium. The sample was mounted on the stub using indium tape. The energy in the XPS spectra was referenced to the adventitious carbon adsorption at 284.6 eV. The shift was cross checked with the position of O 1s from Al $_2$ O $_3$ which is found at 531 eV.

Catalytic activity measurement

The activity of the catalyst was measured in a tubular stainless steel micro reactor. The reactant mixture composition was varied in the range of 0.6–0.8% of CH $_4$ balanced with air at various flow rates. The inlet and outlet mixtures were analyzed using a gas chromatograph equipped with a thermal conductivity detector (TCD) and a concentric-packed single column (Alltech CTR-I). For humid feed experiments, the reactant mixture passed through a saturator and a humidity probe (HumidiProbe, Pico Technology Ltd.) was installed at the outlet. The reaction temperature was measured with a thermocouple placed into the catalyst bed. At constant water vapour pressure, the repeatability of the data is 3.8%.

For catalytic stability studies, a second, separate reactor set-up was used and operated continuously under varying conditions (temperature was increased in order to maintain a 90% level of conversion for methane). Throughout the study, the feed concentrations of methane and carbon dioxide were kept constant at 7000 ppm and 10 000 ppm, respectively. During this experiment, our calculation of the total carbon at the inlet and outlet of the reactor results in an average carbon balance of 96%. The average water content was measured at approximately 85% relative humidity (RH) for the saturator system used ($T = 28^\circ\text{C} \pm 3^\circ\text{C}$, ambient), corresponding to a H $_2$ O $_{(v)}$ pressure of approximately 32 000 ppm. As reported in the literature,⁴ the relative humidity of the VAM stream is fluctuating, ranging from 70% to 100% RH. Thus, our saturator system was aimed at producing humidity within this range. The feed gas hourly space velocity (GHSV) was maintained at 100 000 h $^{-1}$ for the majority of the tests, although in a limited number of tests, the GHSV was varied between 75 000 h $^{-1}$ and 110 000 h $^{-1}$ by manipulating the feed flow-rate. The targeted 90% methane conversion was maintained by increasing the catalyst bed temperature as the catalyst deactivated during time-on-stream.

In order to investigate the effect of the presence of mine dust on the conversion of methane, a 1.0 wt% Pd/Al $_2$ O $_3$

catalyst was mixed with mine dust using the surrogate VAM feed described above, and the reaction was carried out for more than 1200 h of continuous operation. The amount of mine dust mixed into the catalyst is estimated as the quantity of dust deposited for one year of operation (dust loading assumption of 2 mg m $^{-3}$).

Results and discussion

The activity of the catalyst under dry and wet feed

The activity of the 1.2 wt% Pd/Al $_2$ O $_3$ catalyst was measured under alternating dry and wet conditions at a space velocity of 200 000 h $^{-1}$ as shown in Fig. 1. A shift in the T_{90} temperatures (which is a measure of activity) to higher values was observed with the humid compared to dry feed VAM gas. Four alternating cycles of reactions were performed over the same catalyst, highlighting the deactivation phenomenon. For the first cycle under dry feed, complete combustion of methane was obtained at 380 °C. The addition of approximately 3.2 vol% water vapour into the VAM feed slightly reduced the activity of the catalyst within the second cycle experiment. When feed was switched back to dry (cycle 3), the conversion curve overlaps with the 2nd cycle, highlighting the loss of activity under wet feed conditions. Significant deactivation was revealed in the next wet cycle conditions (cycle 4) where complete methane combustion was achieved at temperatures in excess of 470 °C.

Fig. 2 shows the time-on-stream behaviour of 1.2 wt% Pd/Al $_2$ O $_3$ at 320 °C under dry and wet conditions for 12 h. Combustion of 8000 ppm of methane in dry air was changed to wet feed (8000 ppm CH $_4$, 40 000 ppm H $_2$ O and balance air) after 2 h reaction. Once the wet feed was introduced, a sharp decrease in conversion is observed (from *ca.* 90% to 40% conversion). The activity quickly returned to the initial value when the water vapour supply in the feed is turned off, suggestive of a reversible deactivation phenomenon, occurring at least within 2 h oxidation under wet feed conditions.

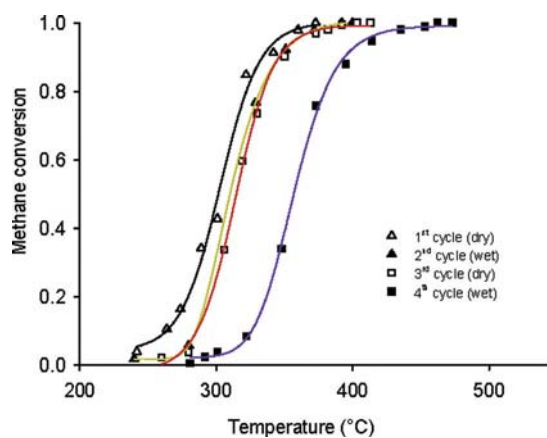


Fig. 1 Methane conversion as a function of reaction temperature of methane oxidation over 1.2 wt% Pd/Al $_2$ O $_3$ catalyst using dry and wet feed. GHSV = 200 000 h $^{-1}$, CH $_4$ inlet = 8000 ppm, wet feed water vapour = 3.2%.

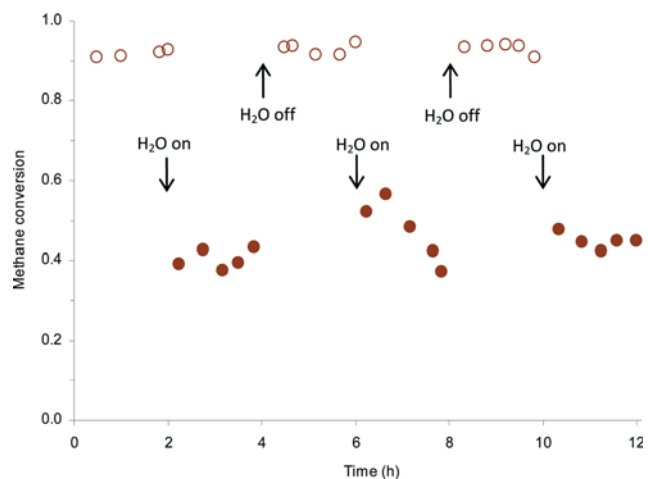


Fig. 2 Time-on-stream evolutions under dry and wet feed over 1.2 wt% Pd/Al₂O₃ catalyst at a temperature of 320 °C. GHSV = 100 000 h⁻¹, CH₄ inlet = 8000 ppm, wet feed water vapour = 3.2%. □ = dry feed, ● = wet feed.

Repeating the jump experiments up to 12 h does not disclose significant loss in activity over a relatively short time period. This behaviour suggests competition for sites between water and methane^{11,18} occurring in this period. Over this relatively short time period, we suggest that species described as responsible for catalyst deactivation such as Pd(OH)₂ are absent, which is supported by our XPS findings (see below).

Our findings are consistent with the results published by others, especially the pulse experiments as reported previously over palladium catalysts^{10,11,19,20} under different reaction conditions. Over 4% Pd/Al₂O₃ catalyst, Burch *et al.*¹⁰ observed reversible deactivation (an instantaneous drop from 40% to nearly 10% conversion at 325 °C) in catalytic activity. Likewise when 2.7% of H₂O was added to 1% methane in an air feed stream, other researchers concluded that the formation of Pd(OH)₂ may not be important since palladium hydroxide under these conditions decomposes at the much lower temperature of approximately 250 °C.²¹ Roth and co-workers¹¹ also observed catalyst deactivation when exposed to a humid feed stream, with a slow initial deactivation stage followed by a dramatic drop in catalyst activity. The same authors suggested that deactivation as a result of feed water vapour is reversible, while water produced in the reaction was suggested to cause irreversible catalyst deactivation. This was concluded from time-on-stream experiments for 6 h and 22 h runs respectively at 350 °C over 1.9 wt% Pd/Al₂O₃ (1% of H₂O was added to 1% CH₄, 4% O₂, balance N₂).¹¹ It was suggested that a progressive transformation of the active phase into the less active phase occurred when water is present as a product.¹¹ In contrast to what is presented in Fig. 2, within 2 h the activity is fairly constant. This is most likely the result of the exposure time of the active Pd sites with wet feed being insufficient to transform PdO into Pd(OH)₂, therefore we do not observe any irreversible deactivation. It also might be a result of the high space velocity we used in our

experiment that the transformation rate of active sites into less active sites is slower compared to what has been reported by Roth and co-workers.¹¹

Stability evaluation of the Pd/Al₂O₃ catalyst

In order to understand the reasons for catalyst deactivation over long periods on stream, a 1.0 wt% Pd/Al₂O₃ catalyst was used continuously for 1150 hours. Prior to the stability test, the activity of this catalyst has been tested and showed similar activities compared with the 1.2 wt% Pd/Al₂O₃ catalyst (see Fig. S1 of the ESI†). The feed composition was 7000 ppm CH₄, 10 000 ppm CO₂, 30 000 ppm H₂O, and balance air where GHSV was in the range of 75 000 h⁻¹ to 110 000 h⁻¹. During the course of these experiments, the furnace temperature was periodically increased, in order to ensure that a conversion level of methane (in excess of 90%) was achieved, mimicking the performance requirements for a large scale catalytic VAM mitigation system.

Fig. 3 shows the methane conversion as a function of reaction temperature for the system over this experimental period. The initial temperature of the system to achieve 90% conversion was 350 °C, with this temperature increasing to 500 °C at a time of 1150 h. A significant rate of deactivation was observed during the first 80 h of reaction. In order to obtain high conversions, the bed temperature was increased from 320 °C to 420 °C during this period, ensuring the targeted 90% conversion level of methane was re-established. The conversion level within the first 200 h of operation exhibits significant variation in activity. This is thought to be due to the initial deactivation phase of the catalyst, which appears to be comparatively fast. This result is detailed further in the ordinate which shows the catalyst bed temperature required to achieve 90% methane combustion conversion. Please note that the reoccurrence of the sharp drop in methane conversion is a result of a longer interval in bed temperature adjustment. The minor fluctuation in the

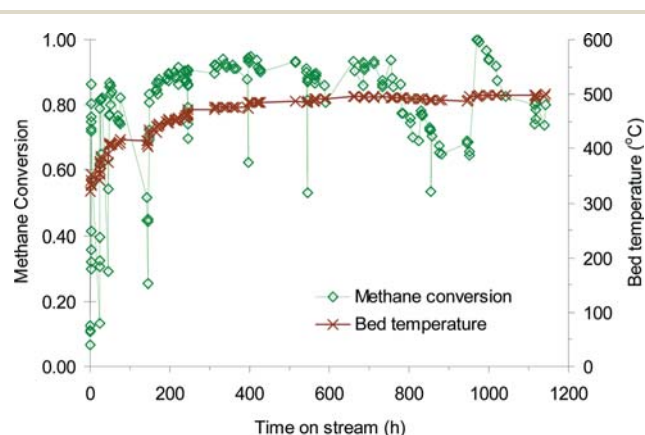


Fig. 3 Time-on-stream fractional methane conversion and corresponding reactor bed temperature over 1.0 wt% Pd/Al₂O₃ catalyst. Feed = 7000 ppm CH₄, 10 000 ppm CO₂, 30 000–40 000 ppm H₂O and balance air. GHSV = 75 000–110 000 h⁻¹. ◇ = methane conversion, × = bed temperature.

methane conversion level observed at a nearly-fixed temperature of the furnace is mainly due to the change in the water vapour concentration which is caused by the change in ambient temperature.

Following the initial deactivation period of the catalyst, methane conversion was maintained at 90%, however it can be seen that after approximately 950 h, the conversion decreases to approximately 70%. At this stage of the time-on-stream experiment, the GHSV was slowly reduced from 100 000 h⁻¹ to 75 000 h⁻¹ whilst maintaining the system temperature.

This was done in an attempt to maintain the targeted 90% methane conversion without having to further increase the catalyst temperature. This test, however, did not have a significant effect on methane conversion. The GHSV was then increased to 110 000 h⁻¹ and the catalyst bed temperature increased to return the system to 90% methane conversion. The catalyst bed temperature tends to plateau in the final stages of the run, suggesting that for long term use a constant temperature can be used to obtain stable conversion.

In order to investigate the long term effect of water produced from the reaction, a VAM experiment under dry feed conditions was carried out for 1600 h where the reactant was 7000 ppm methane and balance air at a space velocity of 100 000 h⁻¹. The variation of the T_{90} temperatures is compared to VAM in a wet feed stream in Fig. 4. Similar to the conversion of a wet VAM feed stream, the temperature required to achieve in excess of 90% conversion of CH₄ (T_{90}) increased over the duration of the experiment. Under wet feed conditions, the experiment was run continuously for a total of 1150 h with a catalyst bed temperature of 500 °C required to achieve 90% methane conversion, while the dry VAM gas feed experiment was run for a total of 1610 h with a final catalyst bed temperature of 450 °C required for T_{90} . To estimate the conversion of methane and in order to assess the influence of the different conditions for the long term, the data for both the dry and wet runs were extrapolated.

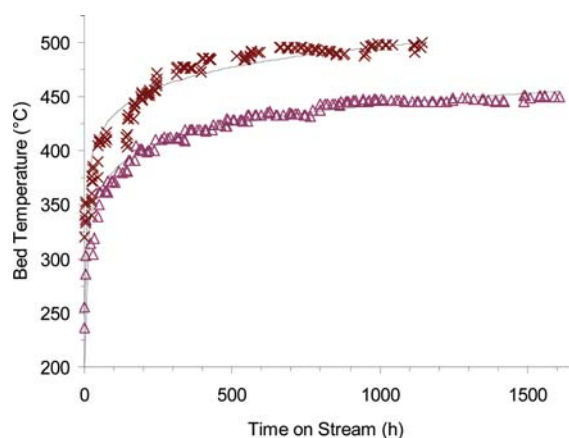


Fig. 4 Catalyst bed temperature required for 90% CH₄ conversion for wet (30 000–40 000 ppm H₂O) and dry time-on-stream runs over 1.0 Pd/Al₂O₃ catalyst. Feed: 7000 ppm CH₄ and balance air, GHSV = 100 000 h⁻¹. × = wet feed run; Δ = dry feed run.

Empirically, a logarithmic function was found to yield the best fit for the experimental data. The estimation results in a final bed temperature of 555 °C for the wet feed and 500 °C for the dry feed over a period of 8760 h (1 year).

The effect of coal mine ventilation air dust on the conversion of methane was assessed and a wet VAM stream was operated continuously for over 7 weeks, where 60.8 mg of VAM dust was packed in front of the 200 mg of catalyst. This quantity of VAM dust corresponds to the amount of dust deposited on the catalyst over a year of continuous operation. Time-on-stream variability and reaction bed temperature over 1.0 wt% Pd/Al₂O₃ catalyst are shown in Fig. 5. The feed was 7000 ppm CH₄, 10 000 ppm CO₂, 32 000 ppm H₂O and balance air at a space velocity of 100 000 h⁻¹. Significantly, higher fluctuations in the conversion levels and temperatures of the bed were observed in these experiments compared to the long term experiments in the absence of dust. This fluctuation is likely a result of the combustion of coal particles present in the VAM dust and channelling with resulting changes in the pressure drop across the catalyst and dust beds (*ca.* 0.1 bar). After *ca.* 700 h on stream, it was noticed that there was a significant decrease in methane conversion. The bed temperature was continually increased to 550 °C over a period of 150 h (time-on-stream, 950 h) in order to restore the conversion level to 90%. As the conversion did not increase, it was suspected that the catalyst bed had shifted slightly into a lower temperature zone of the furnace. The bed was then opened and it was confirmed that the catalyst bed had moved. After that, the catalyst was repacked and the experiment was continued. Subsequent to repacking, the catalyst exhibited similar conversion levels observed before the bed movement. No differences in methane conversion and temperature were observed within the experimental error. This is an experimental artefact due to high volumes of VAM dust, which would not be present in a real VAM mitigation system.

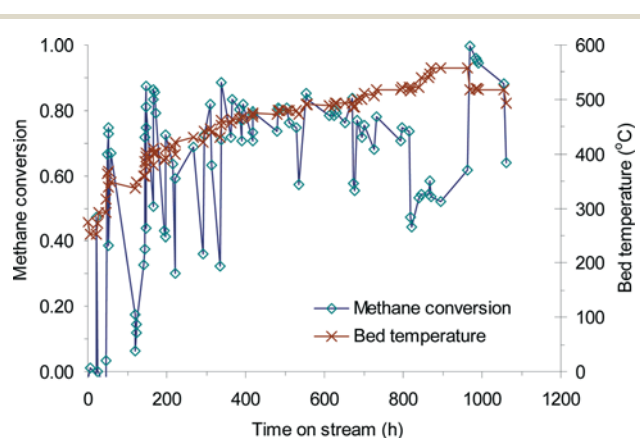


Fig. 5 Time-on-stream evolutions and reactor bed temperature over 1.0 wt% Pd/Al₂O₃ catalyst in the presence of VAM dust. Feed = 7000 ppm CH₄, 10 000 ppm CO₂, 32 000 ppm H₂O balanced air. GHSV = 100 000 h⁻¹. ◇ = methane conversion, × = bed temperature.

Characterization of catalysts

The nitrogen adsorption isotherm experiment results in estimates of the Langmuir surface areas of $98.4 \text{ m}^2 \text{ g}^{-1}$, $92.8 \text{ m}^2 \text{ g}^{-1}$ and $193.4 \text{ m}^2 \text{ g}^{-1}$ for $\gamma\text{-}\delta\text{-Al}_2\text{O}_3$, 1.2 wt% Pd/ $\gamma\text{-}\delta\text{-Al}_2\text{O}_3$, and 1.0 wt% Pd/ $\gamma\text{-Al}_2\text{O}_3$ (commercial catalyst), respectively. Note that the alumina phase used for catalysts prepared in these experiments is somewhat different to what has been used for commercial catalysts, confirmed by our XRD results. The surface area of the commercial catalyst is somewhat higher, although the activity of the catalysts is similar. Thus, as expected, the support surface area appears to have very little influence on catalytic activity. ICP-OES confirms the loadings of 1.0 and 1.2 wt% of Pd on their supports.

The XRD pattern of Pd/ Al_2O_3 catalysts reveal minute reflections attributed to Pd or PdO phases (overlapping with support peaks, thus they are identified by slightly increased intensities and widths of support reflections), consistent with a low net metal loading, and suggests small noble metal particles. The overlap with the support reflections and the small size makes particle size estimation from XRD difficult. As reported in our previous studies, the particle size of the palladium was estimated from the results of pulse H_2 -chemisorption at $109.1 \text{ }^\circ\text{C}$ showing that the average catalyst particle diameter is 12.2 nm , corresponding to a 9.2% level of metal dispersion.²² This particle size estimation agrees with what has been observed with TEM analysis, where particle sizes were measured to vary between 6 and 13 nm .²²

The influence of water vapour adsorption on the active site and the support was investigated using TPD analysis. The intensities of water desorbed from the support material ($\gamma\text{-}\delta\text{-Al}_2\text{O}_3$) and 1.2 wt% Pd/ Al_2O_3 catalysts are plotted in Fig. 6(a) for the fresh active catalyst and Fig. 6(b) for the used catalyst (7 hours at $320 \text{ }^\circ\text{C}$). Prior to water adsorption, fresh catalysts were pre-heated for 1 h at $500 \text{ }^\circ\text{C}$ with a ramp of $5 \text{ }^\circ\text{C min}^{-1}$ and H_2O adsorption was at $110 \text{ }^\circ\text{C}$, while on Pd/ Al_2O_3 (used catalyst) the water was adsorbed during combustion of methane with wet feed at $320 \text{ }^\circ\text{C}$ for 7 h.

In all cases, high and low temperature desorption peaks can be observed. The low temperature peak is observed at

ca. $240 \text{ }^\circ\text{C}$ and the high temperature peak is observed between $350 \text{ }^\circ\text{C}$ and $700 \text{ }^\circ\text{C}$. The low temperature desorption is attributed to weakly bound water, whereas the high temperature peak is attributed to adsorption on coordinatively unsaturated sites.^{23,24}

Over a fresh alumina surface (Fig. 6a), a second desorption peak is observed at *ca.* $600 \text{ }^\circ\text{C}$. On fresh Pd-containing catalysts, the second temperature desorption peak of water is observed at higher temperatures than on the support, indicating that water is more strongly bound on the Pd-containing surface. The higher temperature peak ($600 \text{ }^\circ\text{C}$) observed for the support material shifts to $700 \text{ }^\circ\text{C}$, which suggests either a change in the interaction strength of the sites or structural and chemical changes of the sites by Pd. We suggest that Pd is deposited on sites that can interact strongly with water and transforms into sites that bind even more strongly with water. A small quantity of water is retained on the catalyst at temperatures as high as $700 \text{ }^\circ\text{C}$, similar to what was observed by Mowery and co-workers.¹² This further underscores the formation of catalyst sites interacting strongly with water.

Over the used catalyst (Fig. 6b), the maximum water desorption rate was observed at *ca.* $350 \text{ }^\circ\text{C}$. A quantified amount of water remains on the catalyst at these temperatures (as indicated by the relative area under the peak), suggesting that a significant number of sites are interacting with water to form hydroxides. The desorption peak around $350 \text{ }^\circ\text{C}$ is likely due to water desorption from the hydroxides, consistent with the decomposition temperature of $\text{Pd}(\text{OH})_2$.²¹ The high temperature peak at *ca.* $700 \text{ }^\circ\text{C}$ was not observed, suggesting the absence of sites that are able to strongly adsorb water. Highly coordinatively unsaturated sites could be crucial as sites for oxygen activation and would result in deactivation of the catalyst, similar to what has been suggested in ref. 8. These coordinatively unsaturated sites often are described as edge or corner or surface sites on metal and metal oxides.²⁵ Our estimation of the amount of water adsorbed during experiment is $0.9 \times 10^{-3} \text{ mol g}^{-1}$ and $1.1 \times 10^{-3} \text{ mol g}^{-1}$ for the support and the Pd/ Al_2O_3 catalyst, respectively. The ratio of water desorbed from the catalyst *versus* the amount of Pd is 10, which means the majority of

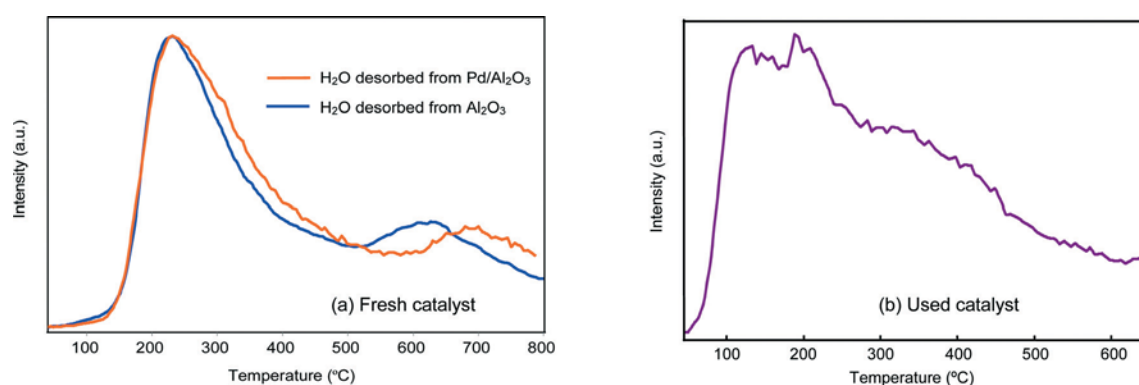


Fig. 6 TPD curves of water desorption from (a) the fresh catalyst (1.2 wt% Pd/ Al_2O_3) and the catalyst support ($\gamma\text{-}\delta\text{-Al}_2\text{O}_3$) from and (b) used catalyst time-on-stream 7 h, Feed: 6000 ppm CH_4 , *ca.* 30 000 ppm H_2O , reaction temperature $320 \text{ }^\circ\text{C}$.

water is adsorbed on the support. However, the presence of palladium on alumina increased the quantity of $\text{H}_2\text{O}_{(v)}$ adsorbed and also resulted in a significant water desorption peak shift toward higher temperatures. This suggests significant interaction of Pd with water.

XPS spectra of activated (calcined-reduced) and used 1.2 wt% Pd/ Al_2O_3 catalyst are displayed in Fig. 7. The binding energies (BE) and Pd/Al ratios are provided in Table 1 for all samples.

XPS spectra of the activated and reduced 1.2 wt% Pd/ Al_2O_3 catalyst (Fig. 7a) revealed two distinct Pd peaks representing the Pd $3d_{5/2}$ core level transitions. The palladium species at 335.0 eV and 336.3 eV can be attributed to Pd^0 and Pd^{2+} , respectively. These species are formed during catalyst activation under air and hydrogen. The presence of metallic Pd and PdO has been determined by comparing the shifts with those reported in the literature.^{3,26,27}

The XPS spectra of the 1.2 wt% Pd/ Al_2O_3 catalyst used for 2 h under dry and wet feed at 335 °C are shown in Fig. 7b. Two species with binding energies (BE) of 335.0 eV and 336.4 eV were observed. The binding energies are similar to the BE obtained from the calcined-reduced sample (Fig. 7a) which suggests little change in the chemical nature of Pd^0 and Pd^{2+} . This observation supported our experimental data presented in Fig. 2 where the loss of activity for 2 h under wet stream is completely reversible and no structural or chemical changes in the catalyst were detected.

Following reaction with lean air–methane mixtures at a temperature of 290 °C for 10 h, the 1.2 wt% Pd/ Al_2O_3 catalyst is deactivated and the XPS spectra of this sample are shown in Fig. 7c. The shape and width of the peak (FWHM = 2.3 eV at Pd $3d_{5/2}$ line) suggests the presence of multiple palladium species. Similar to the spectra of the fresh sample, asymmetry toward higher binding energies indicates that multiple peaks

Table 1 XPS peak positions and Pd/Al ratio

Fig.	Sample	Pd $3d_{5/2}$ peak position (eV)		Pd/Al ratio
		Pd^0	Pd^{2+}	
7a.	1.2 Pd/ Al_2O_3 , calcined-reduced	335.0	336.3	0.0046
7b.	1.2 Pd/ Al_2O_3 , 2 h usage	335.0	336.4	0.0040
7c.	1.2 Pd/ Al_2O_3 , 10 h usage	—	336.0	0.0077
			337.1	
8a.	1.0 Pd/ Al_2O_3 , fresh	334.7	336.1	0.0045
8b.	1.0 Pd/ Al_2O_3 , calcined-reduced	335.2	336.4	0.0045
8c.	1.0 Pd/ Al_2O_3 , 1150 h usage	—	336.3	0.0040
9a.	1.0 Pd/ Al_2O_3 , used in the presence of dust	—	335.9	0.0048
9b.	Dust contaminated with Pd/ Al_2O_3 , used	—	336.2	0.0018

should be fitted. Assuming Gaussian–Lorentzian curves (70% Gaussian), the peak fitting results in two different photoelectron energies at BE of 336.0 eV and 337.1 eV ($3d_{5/2}$ core level). Additional peaks result in little improvement in the χ^2 fit and are thus statistically not significant. The lower energy peak at BE of 336.0 eV is identified as bulk Pd^{2+} as reported in the literature.^{3,27} The presence of PdO corresponds to Pd species identified in Fig. 7a, which indicates transformation of the Pd metal into the oxidized form under reaction conditions. The signal at a higher BE of 337.1 eV can be interpreted as palladium hydroxide (*vide infra*), which appears to be related to the deactivation observed during time-on-stream.

A limited body of research describing hydroxyl compounds was identified, and correlations between progressive alterations in chemical bonding and shifts in XPS binding energies with the nature of hydrogen bonding have been proposed.²⁸ There is a change in the binding energy of $\text{Pd}(\text{OH})_2$ as reported by Barr²⁹ when a hydroxide layer is present on the palladium surface. Experimentally, Barr found that the Pd^0 peak at a BE of 335.4 eV was shifted to 336.9 eV and 338.6 eV upon formation of PdO and $\text{Pd}(\text{OH})_4$, respectively.^{28,29} These shifts in binding energies are similar to what has been observed for Pd $3d_{5/2}$ in our samples (see Fig. 7). The presence of O–H groups on palladium metal can result in a shift of the peak of 1.1 eV toward a higher binding energy. The formation of palladium hydroxide is further substantiated by the re-generation of the active sites when a deactivated catalyst was heated in He (15 ml min^{-1}) at 500 °C for 1 h. H_2 is detected in the exit stream, which most likely originates from the OH groups on the catalyst surface. The TPD spectra plotted in Fig. 6 also support the argument that palladium hydroxide is present in the deactivated sample and is responsible for deactivation.

The spectra of fresh, activated and used samples of the 1.0 wt% Pd/ Al_2O_3 catalyst in the Pd 3d core level region are shown in Fig. 8. For the fresh (as received, Fig. 8a) and activated (calcined-reduced, Fig. 8b) samples, the peak deconvolution results in two species detected at the Pd $3d_{5/2}$ core level. These species are having similar binding energies as reported in Fig. 7a and b.

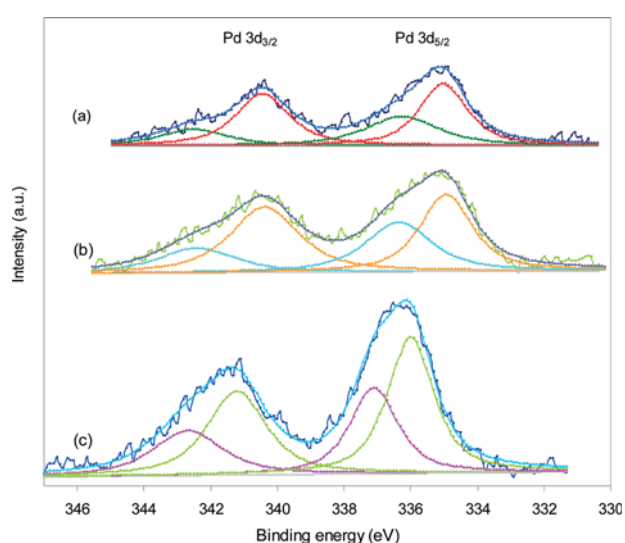


Fig. 7 XPS spectra of the Pd 3d core level of 1.2 wt% Pd/ Al_2O_3 . (a) calcined-reduced sample; (b) used sample of 2 h TOS under humid conditions; (c) used sample of 10 h TOS under humid conditions.

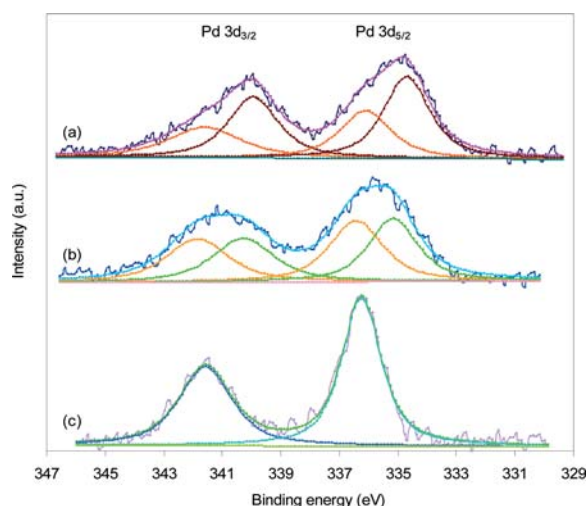


Fig. 8 XPS spectra of the Pd 3d core level of 1.0 wt% Pd/Al₂O₃, (a) fresh sample; (b) calcined-reduced sample; (c) used sample of 1150 h stability test.

Fig. 8c shows the spectra of the used 1.0 wt% Pd/Al₂O₃ catalyst after 1150 h operation using surrogate VAM gas (refer to the catalyst activity data plotted in Fig. 3). XPS analysis of the catalyst discloses a single peak of the Pd 3d_{5/2} core level at 336.3 eV. The presence of a single Pd²⁺ species is proposed as the full width at half maximum of Pd 3d_{5/2} is only 1.8 eV, which is indicative of a single species. Fitting more peaks under Pd 3d spectra does not significantly decrease χ^2 .

XPS spectra in Fig. 8c suggest no palladium hydroxide is present on the catalyst. The increased bed temperature leads to decomposition of hydroxyl species, resulting in a single peak which is interpreted as PdO species dispersed on the support. An increase in Pd crystallite size is suggested to be an important contributor for deactivation as the formation of Pd(OH)₂ was not found, most likely due to the higher temperature.

The accumulation of H₂O on the catalyst increases the surface mobility and results in particle agglomeration as well as potentially hinders the oxygen transfer from the bulk in a Mars van Krevelen type reaction mechanism.⁸ As suggested by Lee and Trimm, thermal deactivation is caused by either sintering of the catalyst or the support material.³⁰ This sintering involves surface/volume diffusion and other transformations. At reaction temperatures close to 0.3 × melting point (Hüttig temperature), the transformation becomes significant.³¹ In our study, after *ca.* 300 h, the bed temperatures were adjusted toward 500 °C close to the Hüttig temperature for Pd at 466 °C, and thus a significant level of sintering would be expected. Please note that the binding energy of the Pd²⁺ of the catalyst used under humid conditions for 1150 h slightly decreases compared to the fresh samples, similar to the catalyst aged in the presence of VAM dust. This is consistent with sintering (see below).

The used 1.0 wt% Pd/Al₂O₃ catalyst from the VAM-dust time-on-stream experiment was analyzed by XPS in order to determine the surface composition of the catalyst and dust

after 1100 h operation. Fig. 9 shows the palladium 3d photoelectron spectra of the used catalyst (a) and used dust mixed with the catalyst (b). The binding energies compiled along with the Pd/Al atomic ratio are provided in Table 1. Deconvolution of the peak at the Pd 3d_{5/2} core level suggests a single peak at a binding energy of 335.9 eV for the used catalyst. This peak is identified as Pd²⁺, which is similar to the species detected from samples in Fig. 7 and 8, and is in agreement with the previous discussion suggesting that palladium oxide is the primary species present on the surface after the long term time-on-stream experiment. Note the decreased binding energy of the used sample (9a) compared to the activated sample (8b). The decreased binding energy can originate not only from the chemical shift but also from final state effects due to relaxation of the core hole. For larger particles, this relaxation effect is less important compared to smaller particles. Thus, the shift can be evidence for larger particles in the used samples, *i.e.*, sintering. Despite a lower intensity, an identical peak is detected also from the XPS spectra of used dust at similar binding energies. As suggested by the overall surface composition of the used catalyst in Table 2, impurities such as Na, Cl and F were also present. It is important to note that the deactivation was little affected by the presence of the VAM dust and these species play a minor role in deactivation.

From the used catalyst, XPS evidence disclosed that *ca.* 0.24% of chlorine deposited on the used catalyst while chlorine was not detected in the fresh catalyst and used dust (see Table 2). Others have suggested that chlorine ions acted as powerful inhibitors during methane oxidation over the supported Pd catalyst^{11,32,33} and removing chlorine from the surface needed a minimum of 10 h reaction time even at temperatures as high as 600 °C.¹¹

Since our reaction temperature is below 550 °C, it appears that chlorine remains on the surface of the catalyst and inhibits catalytic activity. As can be seen in Fig. 5 over a 1100 h reaction, an increase in bed temperature can increase methane conversion. However, it is important to note that in

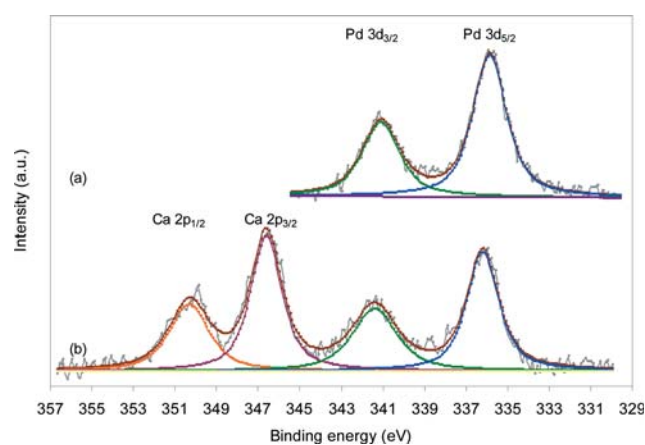


Fig. 9 XPS spectra of the Pd 3d core level of used 1.0 wt% Pd/Al₂O₃ catalyst in the presence of dust, (a) used catalyst; (b) used dust mixed with the catalyst.

Table 2 Surface composition of the used catalyst and a mixture of VAM dust and used catalyst

Sample	Composition (at.%)												
	Pd	O	Al	C	Na	N	Cl	F	Si	Mg	Ca	S	Fe
(a) Used Pd/Al ₂ O ₃ (in the presence of dust)	0.18	57.9	37.2	3.85	0.15	0.22	0.24	0.29	—	—	—	—	—
(b) Used dust + Pd/Al ₂ O ₃ contamination	0.09	43.3	49.1	4.48	0.45	0.33	—	0.22	0.99	0.31	0.44	0.33	—
(c) VAM dust (fresh)	—	39.4	3.2	34.0	0.8	1.4	3.5	—	6.0	5.1	6.2	—	0.4

maintaining an average methane conversion >75% over 1100 h, our reaction temperature does not exceed 600 °C.

Characterization of the VAM dust

The XRD trace of the VAM dust (Fig. S2 of the ESI†) following long term catalytic reaction discloses the presence of calcium carbonate, quartz and iron oxide as distinct phases. Consistent with the phase analysis by XRD, elemental analysis reveals the presence of Ca, Fe and Si (see Table 2). In addition, aluminium, magnesium and titanium were also detected in the samples. These elements may be present as amorphous silicates. Surface analysis by XPS showed a similar composition to that determined by ICP-OES.

XPS analysis of the used catalyst and dust revealed the presence of chlorine on the catalyst. Chlorine can have a significant effect on the activity of the noble metal catalysts and has been detected in the catalyst after 1200 h of reaction. As indicated in Table 2, XPS of the separated VAM dust revealed that chloride was likely removed from VAM gas and deposited on the catalyst surface. Note that complete separation of dust and catalyst was not possible. The presence of Cl in the XPS (Table 2) and its absence in ICP-OES suggest surface enrichment of chlorine on the catalyst that was used in the presence of VAM dust. As already noted, the VAM dust influenced the overall activity (T_{90} at 1100 h was 550 °C compared to the experiment without dust $T_{90} = 500$ °C) but the deactivation was not dramatic. Thus, chlorine does have some impact on the deactivation under our conditions.

Conclusions

The stability of a palladium supported on alumina catalyst has been evaluated during short and long term experiments in the presence of water and VAM dust. Within 2 h, alternating experiments in dry and wet VAM feed suggest *ca.* 50% reversible drop in activity, most likely due to the competition between water and methane to adsorb on the active sites. For short term VAM oxidation, palladium hydroxide was not detected. Prolonged exposure to water leads to the formation of palladium hydroxide and progressively deactivates the Pd/Al₂O₃ catalyst. A long term stability test with humid synthetic ventilation air methane reveals that 90% conversion can be achieved for a period of 1150 h at temperatures ≤500 °C. The water vapour present in the feed stream is the primary factor responsible for catalyst deactivation. Introduction of VAM dust into the reactor leads to some reduced activity most likely due to an inhibition effect of chloride ions on the surface of the catalyst. Nevertheless, in the presence of

ventilation air dust, an average methane conversion higher than 75% can be achieved over 1100 h at a reaction temperature below 600 °C.

Acknowledgements

Financial support from the ACARP is duly acknowledged. A.S. was sponsored by the Provincial Government of Aceh, Indonesia. We thank Jane Hamson for assistance with ICP analysis, and thanks are also due to Jerry P. Li and Viswanathan Arcotumapathy for their help with TPD calibration and chemisorption measurements, respectively. We are grateful to the University of Newcastle for XRD and TEM analyses at EM/X-ray unit, and the Australian Synchrotron for the use of their facilities.

References

- S. Solomon, D. Qin, M. Manning, R. B. Alley, T. Berntsen, N. L. Bindoff, Z. Chen, A. Chidthaisong, J. M. Gregory, G. C. Hegerl, M. Heimann, B. Hewitson, B. J. Hoskins, F. Joos, J. Jouzel, V. Kattsov, U. Lohmann, T. Matsuno, M. Molina, N. Nicholls, J. Overpeck, G. Raga, V. Ramaswamy, J. Ren, M. Rusticucci, R. Somerville, T. F. Stocker, P. Whetton, R. A. Wood and D. Wratt, Technical Summary, *Climate Change 2007: The Physical Science Basis. Contribution of Working Group I to the Fourth Assessment Report of the Intergovernmental Panel on Climate Change*, Cambridge, United Kingdom and New York, NY, USA, 2007.
- H. L. Schultz, P. Carothers, R. Watts and R. McGuckin, *Assessment of the worldwide market potential for oxidising coal mine ventilation air methane*, United States Environmental Protection Agency, Air and Radiation (US-EPA), 2003.
- B. Stasinska, A. Machocki, K. Antoniuk, M. Rotko, J. L. Figueiredo and F. Gonçalves, *Catal. Today*, 2008, **137**, 329–334.
- S. Su, H. Chen, P. Teakle and S. Xue, *J. Environ. Manage.*, 2008, **86**, 44–62.
- S. Su, A. Beath, H. Guo and C. Mallett, *Prog. Energy Combust. Sci.*, 2005, **31**, 123–170.
- I. Karakurt, G. Aydin and K. Aydin, *Renewable Sustainable Energy Rev.*, 2011, **15**, 1042–1049.
- P. Gelin and M. Primet, *Appl. Catal., B*, 2002, **39**, 1–37.
- W. R. Schwartz, D. Ciuparu and L. D. Pfefferle, *J. Phys. Chem. C*, 2012, **116**, 8587–8593.
- F. H. Ribeiro, M. Chow and R. A. Dallabetta, *J. Catal.*, 1994, **146**, 537–544.

- 10 R. Burch, F. J. Urbano and P. K. Loader, *Appl. Catal., A*, 1995, **123**, 173–184.
- 11 D. Roth, P. G elin, M. Primet and E. Tena, *Appl. Catal., A*, 2000, **203**, 37–45.
- 12 D. L. Mowery, M. S. Graboski, T. R. Ohno and R. L. McCormick, *Appl. Catal., B*, 1999, **21**, 157–169.
- 13 D. Ciuparu, N. Katsikis and L. Pfefferle, *Appl. Catal., A*, 2001, **216**, 209–215.
- 14 W. R. Schwartz and L. D. Pfefferle, *J. Phys. Chem. C*, 2012, **116**, 8571–8578.
- 15 G. D. Carlo, G. Melaet, N. Kruse and L. F. Liotta, *Chem. Commun.*, 2010, **46**, 6317–6319.
- 16 H. Yamamoto and H. Uchida, *Catal. Today*, 1998, **45**, 147–151.
- 17 Y. Liu, S. Wang, T. Sun, D. Gao, C. Zhang and S. Wang, *Appl. Catal., B*, 2012, **119–120**, 321–328.
- 18 R. Burch, *Catal. Today*, 1997, **35**, 27–36.
- 19 R. Kikuchi, S. Maeda, K. Sasaki, S. Wennerstr om and K. Eguchi, *Appl. Catal., A*, 2002, **232**, 23–28.
- 20 P. Gelin, L. Urfels, M. Primet and E. Tena, *Catal. Today*, 2003, **83**, 45–57.
- 21 R. J. Card, J. L. Schmitt and J. M. Simpson, *J. Catal.*, 1983, **79**, 13–20.
- 22 A. Setiawan, E. M. Kennedy, B. Z. Dlugogorski, A. A. Adesina, O. Tkachenko and M. Stockenhuber, *Energy Technol.*, 2014, **2**, 243–249.
- 23 X. Liu, *J. Phys. Chem. C*, 2008, **112**, 5066–5073.
- 24 L. B. Backman, A. Rautiainen, M. Lindblad and A. O. I. Krause, *Appl. Catal., A*, 2009, **360**, 183–191.
- 25 G. Busca, in *Metal Oxides: Chemistry and Applications*, ed. J. L. G. Fierro, CRC Press, Taylor & Francis Group, Boca Raton, 2006, p. 247.
- 26 K. Yasuda, T. Masui, T. Miyamoto and N. Imanaka, *J. Mater. Sci.*, 2011, **46**, 4046–4052.
- 27 A. V. Naumkin, A. Kraut-Vass, S. W. Gaarenstroom and C. J. Powell, 2012.
- 28 S. J. Kerber, J. J. Bruckner, K. Wozniak, S. Seal, S. Hardcastle and T. L. Barr, The nature of hydrogen in x-ray photoelectron spectroscopy: General patterns from hydroxides to hydrogen bonding, *J. Vac. Sci. Technol., A*, 1996, **14**, 1314–1320.
- 29 T. L. Barr, *J. Phys. Chem.*, 1978, **82**, 1801–1810.
- 30 J. H. Lee and D. L. Trimm, *Fuel Process. Technol.*, 1995, **42**, 339–359.
- 31 D. L. Trimm, in *Studies in Surface Science and Catalysis*, ed. H. B. Calvin and B. B. John, Elsevier, 1991, vol. 68, pp. 29–51.
- 32 D. O. Simone, T. Kennelly, N. L. Brungard and R. J. Farrauto, *Appl. Catal.*, 1991, **70**, 87–100.
- 33 D. Gao, S. Wang, C. Zhang, Z. Yuan and S. Wang, *Chin. J. Catal.*, 2008, **29**, 1221–1225.